ANTIMICROBIAL PEPTIDE RESISTANCE AND IMMUNOMODULATION BY HIV-1 GP41

by

MATTHEW PRICE WOOD
M.S, University of Central Florida, 2010

A dissertation submitted in partial fulfillment of the requirements
for the degree of Doctor of Philosophy
in the Burnett School of Biomedical Sciences
in the College of Medicine
at the University of Central Florida
Orlando, Florida

Spring Term
2014

Major Professor: Alexander M. Cole

ABSTRACT

Fusion inhibitors are a class of antiretroviral drugs used to prevent entry of HIV into host cells. Many of the fusion inhibitors being developed, including the drug enfuvirtide (ENF), are peptides designed to mimic, and thereby competitively inhibit, the viral fusion protein gp41. An exception to this is a class of cyclic, cationic, antimicrobial peptides known as θ-defensins, which are produced by many non-human primates and exhibit broad-spectrum antiviral and antibacterial activity. Currently, the θ-defensin analog RC-101 is being developed as a microbicide to prevent sexual transmission of HIV-1. Understanding potential RC-101 resistance, and how resistance to other fusion inhibitors affects RC-101 susceptibility, is critical for future development.

Partial drug resistance due to genetic variability within HIV-1 presents a major hurdle in microbicide development. Drug-resistance mutations, whether naturally occurring or resulting from selection during treatment, often apply to many drugs in a particular class. Combining different drug classes into a single microbicide should provide greater protection against the growing variability observed in HIV. Our work has identified the beneficial effects of combining the fusion inhibitor RC-101 and the RT inhibitor CSIC to prevent transmission of clinically isolated and drug-resistant HIV-1.

Several aspects of HIV-1 virulence and pathogenesis are mediated by the envelope protein gp41. Additionally, peptides derived from the gp41 ectodomain have been shown to induce chemotaxis in monocytes and neutrophils. While this chemotactic activity has been

characterized, it is not known how these peptides could be produced under biological conditions. Our findings demonstrate that the epithelial serine protease matriptase efficiently cleaves the gp41 HR1 region at conserved residues into a chemotactic peptide.

Here, we present evidence that advances our understanding of resistance to peptide entry inhibitors, reveals a potential benefit to combining specific drugs in an antiviral microbicide, and identifies a pathway by which HIV-1 may generate peptides to exploit host immunity. This work thereby facilitates improved methods in countering drug resistance and the development of new antiviral approaches to prevent HIV-1 transmission. Additionally, we have revealed basic mechanistic evidence that shed light on our current understanding of HIV-1 infection. Specifically, our focus on gp41 provides much needed insight into its role in membrane fusion, drug susceptibility, and modification of host responses.

For Michele and Jonas

ACKNOWLEDGMENTS

I would first like to individually acknowledge my committee members, Drs. Karl Chai, Li-Mei Chen, Kenneth Teter, and Chris Parkinson for their guidance over the years. Drs. Chai and Chen, thank you for taking a chance and allowing me to work in your laboratory as an undergraduate and assigning me to work with an excellent Ph.D student like Mengqian "Max" Chen. Dr. Teter, your classes sparked my interest in infectious disease research and I appreciate the friendly and helpful discussions we have had over the years. Dr. Parkinson, you taught me how to think differently about biology in a way that has, and will continue to, influence my research.

Of course, this body of work would not be possible without the patience and guidance of my advisor, Dr. Alexander Cole. Your support over the years has allowed me to develop the creativity, resilience, and attention to detail that I will bring wherever my research takes me. Most importantly, you allowed me to make mistakes, from which I learned the most valuable lessons that assist me both in and out of the lab.

My experience would also be incomplete without the hands-on training that I received working with Dr. Amy Cole. In addition to basic skills to serve me at the bench, Amy taught me valuable lessons in experimental design and how to think clearly about what variables were important, and why. This knowledge and experience has allowed me to develop entirely new methods over the years as well as troubleshoot existing ones to fit the requirements of the project.

I would also like to thank all of my labmates, past and present, for their friendship and support. In particular, Colleen Eade, Gowrishankar Muthukrishnan, Nicole Cowan, Ryan Lamers, and Christine Chong. I was fortunate to be here with you all and I could not ask for better co-workers and friends.

Lastly, I would like to thank my wife Michele Costello. This work never would have materialized without her support and understanding over the years.

TABLE OF CONTENTS

LIST OF FIGURES

LIST OF TABLES

LIST OF ABBREVIATIONS

CSIC	5-chloro-3-phenylsulfonylindole-2-carboxamide
ENF	Enfuvirtide
FPR1	Formyl Peptide Receptor 1
FPR2	Formyl Peptide Receptor 2
gp120	Glycoprotein 120
gp41	Glycoprotein 41
HIV	Human Immunodeficiency Virus
HR1	Heptad Repeat 1
HR2	Heptad Repeat 2
MALDI TOF	Matrix-Assisted Laser Desorption/Ionization Time of Flight
NNRTI	Non-Nucleoside Reverse Transcriptase Inhibitor
PCR	Polymerase Chain Reaction
RC-101	Retrocyclin-101
RLU	Relative Light Unit
RT	Reverse Transcriptase

CHAPTER 1: INTRODUCTION

HIV/AIDS and Microbicides

After three decades of research, HIV/ AIDS remains as one of the leading global pandemics. According to the WHO and UNAIDS, in 2012 roughly 35.3 million people were living with HIV and 1.6 million people died that same year due to AIDS-related illnesses. While antiviral strategies, such as Highly Aggressive Antiretroviral Therapy (HAART) have made HIV-1 all but a livable infection, vaccination attempts have yet to prove successful and transmission continues with over two million new infections in 2012 [1]. For this reason, improved antiviral prophylaxis methods are being pursued as a solution that could significantly reduce HIV transmission and ultimately reduce the number of AIDS associated deaths.

Early attempts at an anti-HIV microbicide generally consisted of acidic formulations, designed to lower the pH of the vaginal milieu and thereby directly inactivating HIV-1, and employing a variety of surfactants to disrupt the HIV-1 lipid envelope [2,3]. While such strategies were shown to be effective in preventing HIV-1 infection in a variety of *in vitro* studies, these treatments were often neutralized or degraded by the dynamic vaginal environment. Later, sulfated polyanionic or polysaccharide compounds were formulated as microbicides designed to coat mucosal surfaces and protect target cells from infection [4,5]. While preclinical data appeared promising, effective in vivo protection could not be achieved in phase III clinical trials [5,6]. With the disappointment of previous attempts at microbicide development, it has become evident that microbicides should work through safe, specific, and potent mechanism-based approaches, rather than the previously attempted non-specific

compounds, so as to provide directed protection against viral infection while minimally affecting the contacted tissue. Such mechanistically based microbicides will require us to draw upon our ever-growing understanding of the biology of HIV-1 and, in particular, how the virus infects host cells, modifies the host immune system, and evolves resistance to current antiviral drugs.

HIV-1 Entry and gp41

HIV-1 is an enveloped virus that binds to, and fuses with, CD4+ leukocytes within a human host. Protein "spikes" coating the viral envelope mediate this process. The spikes are composed of a stable trimer of virus proteins gp120 and gp41. Entry is initiated when gp120 binds to CD4 on the surface of the susceptible host cell. Binding to CD4 brings the virus into close proximity with the host cell membrane permitting gp120 to bind to a coreceptor, such as CCR5 or CXCR4 [7]. This step induces changes in the envelope spike allowing gp41 to insert itself into the lipid bilayer of the host membrane, thus starting the fusion process. Each gp41 molecule in the envelope trimer consists of two alpha-helical regions, heptad repeats 1 and 2 (HR1 and HR2), a disulfide loop region, and an intracellular domain extending into the viral envelope. Following insertion of gp41 into the host membrane, the HR1 and HR2 helices form a stable leucine zipper structure, pulling the viral envelope into the host membrane causing membrane fusion. After fusion, the HIV-1 capsid escapes into the cytosol and disassembles, allowing single stranded, negative sense viral RNA to be reverse-transcribed into single stranded DNA by virally encoded reverse transcriptase (RT). RT also has the ability to synthesize a complementary DNA strand to form the complete double stranded DNA viral genome. Virus

DNA is then integrated into host genomic DNA by HIV-1 integrase, completing the initial infection [8].

Fusion Inhibitors and Retrocyclin

As a critical stage in infection, HIV fusion has more recently become a target for several new compounds known collectively as fusion inhibitors. These drugs exploit conformational changes in gp41 that provide a kinetic window for binding to the gp41 ectodomain [9,10]. An important advantage of a drug that targets fusion, rather than earlier stages in entry, is that viral tropism and the highly variable gp120 sequence rarely affect the anti-HIV activity of these drugs. This is supported by reports that peptides targeting fusion have been shown to be active against a more diverse group of primary HIV isolates of varying subtypes and tropisms [11-14]. One such drug, enfuvirtide (ENF), is an anionic, 36-amino acid peptide that competes with the HR2 region of gp41 for binding to HR1, thus preventing formation of the mature gp41 6-helix bundle required for fusion [15]. Currently, enfuvirtide (ENF) is the only fusion inhibitor approved for HIV-1 treatment, and resistant viruses continue to emerge [16,17].

HIV-1 fusion is also the primary target of the primate host defense peptides known collectively as θ-defensins [9,18]. Theta-defensins likely bind to the C-terminal α-helix of gp41, thereby preventing formation of the 6-helix bundle structure that mediates membrane fusion [9,19]. Research on θ-defensins as fusion inhibitors has focused primarily on retrocyclin, a θ-defensin derived from a human pseudogene, and its synthetic analogs. Retrocyclins have been found to inhibit HIV-1 infection in both in vitro and in ex vivo models and have been shown to exhibit antiviral activity against both R5 and X4 tropic clinical isolates of HIV-1 [20,21].

Retrocyclins have also been shown to overcome drug resistance mutations in gp41 through only a two-fold increase in peptide concentration [18]. In addition to their anti-HIV activity, retrocyclins are not cytotoxic at relatively high concentrations and do not elicit a host response while remaining active in both organotypic tissue and non-human primate models [22,23]. Because of its unique stability and safety, combined with its potent anti-HIV activity, even in the presence of mucosal fluids, the retrocyclin analog RC-101 is currently being researched for its potential as an intravaginal HIV-1 microbicide.

Viral Transmission and Chemotaxis

Transmission of HIV-1 occurs at mucosal surfaces where epithelial cells, under normal conditions, form a protective barrier against pathogens. Several models have been proposed to explain how HIV-1 is capable of penetrating this barrier to infect CD4 positive leukocytes [24]. These include direct contact with virus at the mucosal surface with resident Langerhans dendritic cells and abrasions in the squamous epithelial layer which allow penetration of virus into deeper tissues. CD4 positive cells may also be recruited to sites of infection as responders to chemotactic stimulation by inflammatory cytokines or other factors [25]. The CCR5-expressing monocytes and macrophages are some of the first cells to migrate into tissue at the site of infection. R5-tropic HIV, which utilizes CCR5 for entry, is predominantly responsible for infection of a new host during transmission [26]. Together, this evidence supports a model where chemotactic stimuli induce migration of monocytes, macrophages, or dentritic cells to the site of HIV-1 infection where the virus can infect prior to dissemination in the lymph nodes and infection of CD4+ T-cells. Understanding the mechanism by which HIV-1 may modify the

host's innate immunity to induce migration of susceptible cells will aid in the development of new and effective antiviral strategies.

CHAPTER 2: A COMPENSATORY MUTATION PROVIDES RESISTANCE TO DISPARATE HIV FUSION INHIBITOR PEPTIDES AND ENHANCES MEMBRANE FUSION

Introduction

Prevention of HIV transmission using safe and effective treatments with specific mechanisms of action remains a necessary challenge in the development of microbicides. Of the options currently being explored, HIV entry has become an attractive target for HIV treatment and prevention. Entry is a multi-step process in which interactions between viral and host proteins result in fusion of the enveloped virus with host membranes. Fusion of the host and viral membranes occurs through direct insertion of gp41 into the host membrane and subsequent formation of a trimer of gp41 hairpin complexes, composed of the heptad repeat regions 1 and 2 (HR1 and HR2). The formation of this stable complex, referred to as a 6-helix bundle, brings the viral and host membranes into close enough proximity for fusion to occur [27,28].

During membrane fusion, conformational changes in the envelope proteins provide a kinetic window for inhibition by drugs that bind to the gp41 ectodomain [9,10]. One such drug, enfuvirtide (ENF), is an anionic, 36-amino acid peptide that competes with the HR2 region of gp41 for binding to HR1, thus preventing formation of the mature gp41 6-helix bundle required for fusion [15]. Currently, enfuvirtide (ENF) is the only fusion inhibitor approved for HIV treatment, and resistant viruses continue to emerge [16,17].

Another class of antiviral peptides that has been shown to act as fusion inhibitors are retrocyclins [9,19,29]. These are synthetic, 18-residue, cyclic antimicrobial peptides that

possess amino acid compositions and structures based on the theoretical product of human θ-defensin pseudogenes. Retrocyclins have been found to inhibit HIV-1 infection in both *in vitro* and in *ex vivo* models and have been shown to exhibit antiviral activity against both R5 and X4 tropic clinical isolates of HIV-1 [21,30]. Retrocyclins have also retained their antiviral activity for over 1 week following application in non-human primates [31]. Further, retrocyclins remain stable under acidic conditions, are resistant to boiling, and lack cytotoxic and proinflammatory activity at concentrations over 100 times their IC_{50} [32,33]. Because of its unique stability and safety, combined with its potent anti-HIV activity even in the presence of mucosal fluids, the retrocyclin analog RC-101 is currently being developed as an intravaginal microbicide to prevent sexually transmitted HIV-1.

Retrocyclins prevent viral membrane fusion by binding the HR2 helix of gp41 [9,19]. Using multi-round, serial passaging of the HIV-1 R5 strain, BaL, in the presence of sub-inhibitory concentrations of the RC-101, we selected for partially resistant mutants. In agreement with retrocyclins preventing gp41 activity, mutations in gp41 alone were shown to be sufficient for RC-101 resistance in pseudotyped viruses. These mutations identified in gp41 were Q66R and N126K, located in the HR1 and HR2 regions, respectively [29]. Due to the cationic nature of these mutations, it was presumed that they might act to electrostatically repel the cationic RC-101 peptides.

Here, we sought to delineate the mechanism by which mutations in gp41 contribute to RC-101 resistance. Specifically, we determined that Q66R compromises gp41 fusion and entry kinetics, and that N126K behaves as a compensatory mutation to enhance gp41 activity in RC-101 resistance, as has been observed in resistance to ENF [34]. This is the first time that

mutations compromising gp41 activity, followed by a compensatory mutation, have been observed as a pattern of drug resistance used to evade a non-gp41-mimetic peptide. Additionally, we identified the activity of RC-101 against clinically relevant enfuvirtide-resistant mutants.

Materials and Methods

BaL env Molecular Clones and DNA Constructs

The pNL43 plasmid encodes an infectious X4 strain of HIV-1 [35]. Briefly, pNL43 was digested using EcoR1 and XhoI prior to gel purification of the 11 kb cleavage product using the QIAEX II system (Qiagen, Valencia, CA). For the construction of infectious molecular clones containing the BaL *env* sequence, viral RNA was isolated from infected PM1 cell supernatants containing high titers of BaL as determined by gag p24 concentration using a p24 ELISA (Perkin-Elmer, Waltham, MA). Viral cDNA was generated from purified RNA using the Superscript III system (Life Technologies, Carlsbad, CA). *env*-containing regions were enriched using oligonucleotide primers (FWD 5'-CTGCAACAACTGCTGTTTATCC-3' REV 5'-GATACTGCTCCTACTCCATCTGCT-3') designed to target the 3' region of *vpu* and the 5' region of *nef*. Cloning inserts were then purified from PCR products using crystal violet gel purification with QIAquick columns (Qiagen). Purified DNA was then inserted into the TOPO-XL cloning vector and sequenced using the M13F and M13R priming sites as well as *env*-specific sequencing primers [29]. After sequencing, *env* inserts were prepared for InFusion cloning by adding EcoRI and XhoI –specific extensions in a second round of amplification (FWD 5'-

GCCATAATAAGAATTCTGCAACAACTGCTGTTTATCC-3' REV 5'-TTTTCTAGGTCTCGAGATACTGCTCCTACTCCATCTGCT-3'). The BaL *env*- containing PCR product was then cloned into the pNL43 plasmid backbone using the InFusion cloning system (Clontech, Mountain View, CA). This method was employed to avoid complications due to non-conserved restriction sites between pNL43 and BaL, thus preserving the complete BaL *env* sequence. The pMONO-neo GFP vector (Invivogen, San Diego, CA) was transfected into 293T cells and used for visualization of cell-cell fusion.

Virus and Cell Culture

The following cell lines were obtained from the NIH AIDS Research and Reference Reagent Program, Division of AIDS, NIAID, NIH: TZM-bl from Dr. J.C. Kappes (University of Alabama, Birmingham, AL) and Dr. X. Wu (University of Alabama, Birmingham, AL and Tranzyme, Research Triangle, NC) and PM1 cells from Dr. M. Reitz (Institute of Human Virology, Baltimore, MD). 293T cells were purchased from the American Type Culture Collection (ATCC). TZM-bl reporter cells and 293T cells were maintained in DMEM supplemented with 10% fetal bovine serum with penicillin and streptomycin. PM1 cells were maintained in RPMI 1640 media supplemented with 20% fetal bovine serum with penicillin and streptomycin. Cells were stored at 37 °C and 5% CO_2. Virus from molecular clones was produced by transfecting 293T cells with viral DNA using the Effectene (Qiagen) following the manufacturer's instructions. Viral 293T supernatants were collected 24 hours after transfection and immediately stored at -80 ºC.

Antiviral Peptides and Synthesis

The 18 amino acid RC-101 peptide was synthesized as previously described [29,36]. ENF was provided by the NIH AIDS Research and Reference Reagent Program (Trimeris/Roche) and was reconstituted in water prior to storage at -20 ºC. The α-defensin HNP-1 was purchased from Bachem (Torrance, CA) and was reconstituted in water prior to storage at -20 ºC. HIV inhibitory peptides Grifonin-1 and RC107GG-F2 were produced by solid-phase FMOC chemistry as previously described [37,38].

Antiviral Activity Assays

TZM-bl luciferase reporter cells were used to determine inhibition of infection as previously described [29]. TZM-bl cells were plated in 96-well, black, transparent bottomed plates at a density of 5×10^4 cells per well in 100 µL of the previously described culture media. 24 hours after plating, media was removed and replaced with peptide or vehicle control in 50 µL culture media before incubation for 10 minutes at 37 ºC and 5% CO_2. Viral stocks were titered using β-galactosidase expression in TZM-bl reporter cells infected with serial dilutions of wild-type and mutant HIV-1 molecular clones using a modified MAGI cell assay [39]. Briefly, TZML-bl cells were plated at 1.0×10^3 cells/well in a 96-well dish prior to 24-hour incubation. Cells were then infected in quadruplicate with dilutions of viral stocks ranging from 4^{-3}- 4^{-12}. After 48 hours of infection, cells were washed, fixed, and stained with Xgal for β-galactosidase activity. Infected blue cells were counted in each dilution and TCID50 values were then calculated using the method of Reed and Muench [40]. In experiments with antiviral compounds, virus was used at MOI 0.2 for each viral genotype tested. In experiments using

HNP-1, Grifonin-1, and RC107GG-F2, serum-free conditions were used for the initial 4 hours of infection, before replacement of media with DMEM supplemented with 10% FBS, in order to observe antiviral activity. Infected cells were incubated for 24 hours before removal of media and lysis using Glo-Lysis buffer (Promega, Madison, WI). Plates containing lysed cells were sealed in parafilm and stored at -80 ºC for 1 to 24 hours before thawing and treating with 100 µL per well of Bright-Glo reagent (Promega). Bioluminescence was measured using an Lmax luminometer (Molecular Devices, Sunnyvale, CA). RLUs were normalized to baseline expression in uninfected cells.

Viral Fitness Assay

PM1 infections were carried out in 100 µL of previously described culture media in deep 1ml volume 96-well plates. 1×10^5 PM1 cells were incubated with peptide or vehicle control for 10 minutes before infection using an MOI of 0.003. Cells were then incubated at 37ºC and 5% CO_2 for 2 hours, agitating every 30 minutes. Conditions with virus and peptide or with vehicle control were diluted with the addition of 900 µL culture media to each well. Treated cells were then centrifuged 200×g for 5 minutes. Media containing virus and peptide or control was aspirated and cell pellets were re-suspended in 0.5 ml culture media containing peptide or control at experimental concentrations. Media treated with drugs or vehicle controls was changed on days 3 and 5 with the volume of cultures being increased to 1 ml on day 3. Supernatants were collected on day 7 and stored at -80 ºC. Levels of p24 in samples were determined using an HIV-1 p24 ELISA.

Cell-Cell Fusion Assay

Fusion efficiency of wild type and mutant envelope proteins was determined using a cell-cell fusion assay consisting of Env- and GFP-expressing 293T effecter cells and luciferase-expressing TZM-bl reporter cells. 293T cells were transfected with equivalent molar concentrations of both molecular clones and GFP or GFP alone in 24-well dishes. The protease inhibitor saquinavir was used at 1 µM concentrations to prevent virion maturation while allowing envelope expression and processing in effector cells. Twenty-four hours after transfection, 293T cells were washed, trypsinized, and co-cultured with TZM-bl cells using a 1:1 ratio of 2×10^4 cells each in black 96-well plates. After 6 hours of co-culture, cells were lysed and stored at -80 ºC overnight. Luminescence was measured using an Lmax luminometer (Molecular Devices). Alternately, transfected cells were co-cultured with TZM-bl cells grown on 8 well chamber slides (Lab-Tek, Bloomington, IN) for 6 hours before fixing with 4% paraformaldehyde and washing twice with PBS. Coverslips were mounted on fixed cells using DAPI-containing mounting solution (Vector Laboratories, Burlingame, CA). Images were acquired using a Zeiss Axiovert inverted fluorescent microscope with Axiovision software.

Determination of Entry Kinetics

TZM-bl reporter cells were plated in black 96-well plates at 2.5×10^4 cells per well. After 24 hours, cell supernatants were removed and replaced with 50 µl fresh media. Suspensions of equivalent concentrations of tested virus were quickly added to each well before centrifugation of plates at 2095×g for 30 minutes at 4 ˚C as previously described [41]. Plates were then kept at 37 ºC for 0-1 hour, and infection was stopped at individual time points by adjusting the

concentration of ENF in experimental wells to 5 μg/ml. This concentration was found to not affect cell metabolism via MTT assay. Plates were incubated for 24 hours before lysing cells and measuring bioluminescence as described above.

DNA Sequence and Protein Structural Analysis

Mutations in gp41 were observed and confirmed using eBioX Software for Mac OSX to generate alignments and concatenate Sanger Sequencing data. Structural analyses of gp41 mutations were carried out using Mac PyMOL (DeLano Scientific).

Statistical Analysis

All analyses were performed using GraphPad Prism v4.0c. TZM-bl antiviral assays were analyzed using an unpaired student's t-test or two-way ANOVA with bonferroni correction. Viral fitness assays and differences in cell-cell fusion were analyzed using a paired student's t-test to account for inter-assay variability. Differences in entry kinetics were determined using linear regression to compare slopes.

Results

RC-101 selects for enfuvirtide-resistant HIV-1

Infectious molecular clones containing the complete BaL R5 envelope gene were produced using InFusion cloning. This method utilizes 15 base pair single-stranded DNA present at the 5' ends of the insert and vector DNA, which allows cloning of PCR products into plasmids

based on areas of homology (**Figure 1A**). This allowed cloning of BaL *env* into the pNL43 vector despite differences in restriction enzyme recognition sites. Chimeric BaL-pNL43 HIV-1 constructs (pNBaL) were generated containing both the wild type and RC-101-passaged *env* genes. The molecular clone produced from the RC-101-passaged *env* (referred to as RCres) contained the gp41 mutations Q66R and N126K, in addition to several mutations in the variable regions of gp120.

Equivalent amounts of virus, as determined using p24 proteins levels, were used to infect TZM-bl cells in the presence or absence of increasing concentrations of both RC-101 and ENF or a vehicle control (**Figure 1B and 1C**). Wild type pNBaL was almost completely inhibited by RC-101 at 10 μg/ml and by ENF at 200 ng/ml. Mutant pNBaL containing multiple *env* mutations showed significant resistance to both drugs at varying concentrations and was inhibited by approximately 50% by both RC-101 at 10 μg/ml and ENF at 200 ng/ml.

While RC-101 and ENF are structurally and chemically disparate drugs, these results demonstrate that a mutant virus selected by RC-101 also displays partial resistance to ENF. This could be explained by the presence of the N126K mutation in the HR2 region of the RC-101-resistant virus. Previously, this amino acid mutation in HR2 has been found to occur with the ENF mutation V38A in HR1, where it has been attributed to an increased rate of fusion and a potential reduction in the kinetic window in which ENF, and presumably other gp41-mimetic peptides, can exert their activity [34,42]. Individual mutations within the RC-101-resistant gp41 would have to be explored further in order to explain the observed cross-resistance.

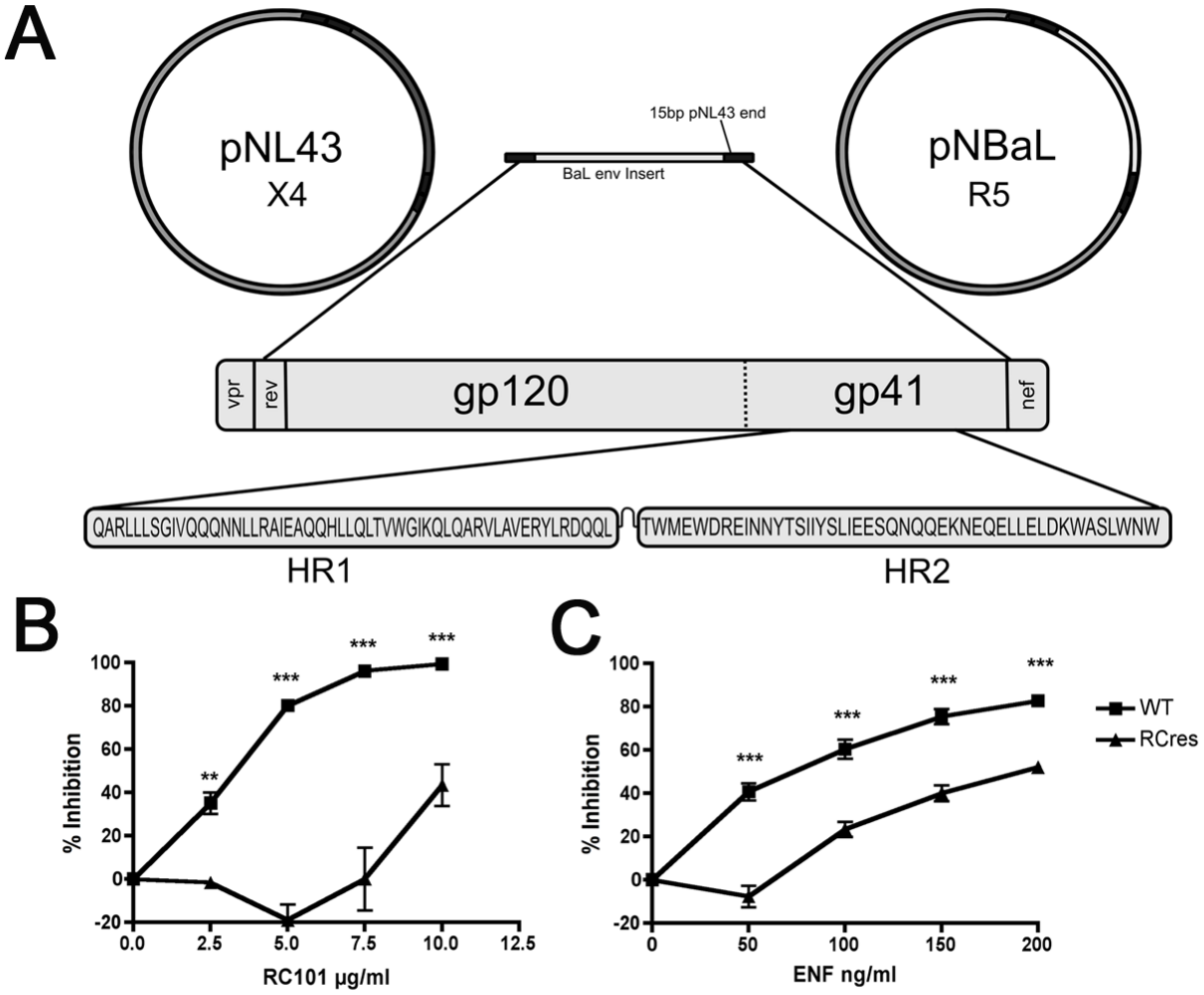

Figure 1: Synthesis and Characterization of BaL *env* Molecular Clones.

(**A**) To study the effect of gp41 mutations identified in the BaL envelope, the dominant *env* genotypes from untreated and RC-101-passaged virus were used to generate the pNBaL molecular clone containing the complete BaL envelope within pNL43. Molecular clones possessing the envelope proteins cloned from untreated BaL (WT) or from RC-101-passaged BaL (RCres) were treated with either (**B**) RC-101 or (**C**) ENF. Error bars represent SEM. Differences in percent inhibition were determined between WT and RCres at each drug concentration (N=3; **=p<0.01, ***=p<0.001).

Resistance mutations in HR1 are drug-specific while an HR2 mutation provides variable cross-resistance

To determine which specific mutations contributed to drug resistance, we introduced the two gp41 mutations observed in RC-passaged BaL, Q66R and N126K, into the wild-type BaL *env*. We also generated mutants containing the well-characterized ENF resistance genotypes V38A and V38A+N126K. These mutants were used to infect TZM-bl reporter cells at MOI 0.2, in the presence and absence of either RC-101 or ENF at varying concentrations.

As expected, the wild-type virus exhibited susceptibility to both RC-101 and ENF (**Figure 2A and 2B)** The Q66R mutant demonstrated resistance to RC-101, with an IC50 2.3-fold higher than the wild-type virus. At the same time, the IC50 of ENF against Q66R was 2.3-fold lower than the wild-type virus. The Q66R+N126K double mutant possessed greater resistance to RC-101 than the wild-type virus (3.1-fold) and than Q66R alone (1.4-fold). Q66R+N126K also demonstrated increased infection at 10 μg/ml versus control conditions, but could be inhibited >80% at 20μg/ml. These observations suggest that the addition of N126K improves resistance to RC-101.

Conversely, the V38A mutant was resistant to the highest concentrations of ENF tested, yet remained susceptible to RC-101. The V38A+N126K double mutant was also resistant to ENF at all concentrations tested, and additionally demonstrated 1.6-fold greater resistance to RC- 101 than the wild-type virus. The HR1 mutations Q66R and V38A were analyzed using the theoretical structure of the mature gp41 protein and both were found to be present on the same region of the HR1 helix responsible for the intramolecular association with HR2 (**Figure 2C and 2D**) [43]. While both mutations appeared at the same region of the HR2 helix, V38A and

Q66R are located near the N and C termini of HR1, respectively, potentially contributing to the specificity for either drug tested.

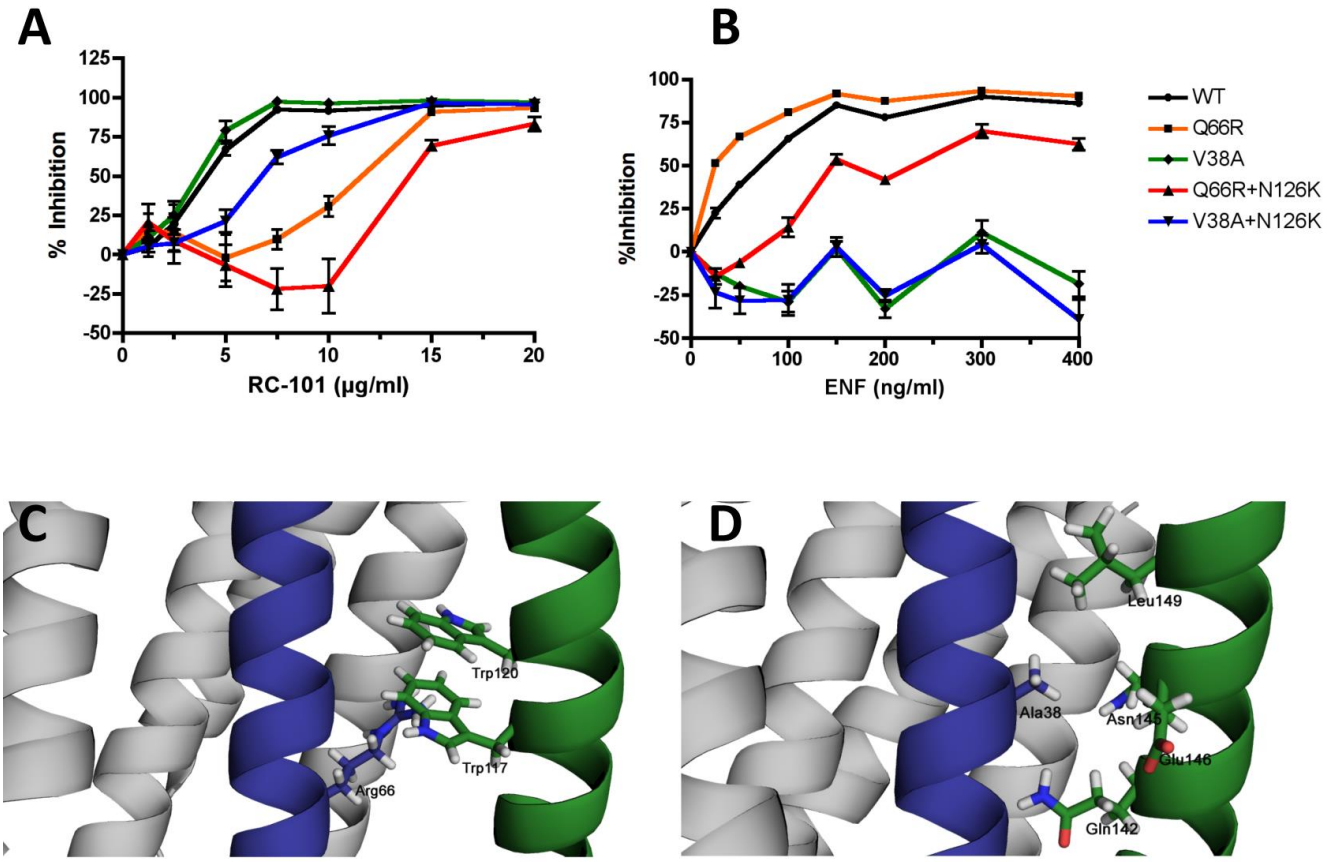

Figure 2: Effect of HR1 and HR2 Mutations on Drug-Resistance.

The role of individual gp41 mutations on drug-resistance was determined using site-directed mutagenesis of the pNBaL vector. The gp41 mutations identified in RC-101 resistant virus, Q66R and Q66R+N126K, were used to understand contributions to drug resistance. We also tested mutations shown to confer resistance to ENF, V38A and V38A+N126K. (**A+B**) Equal concentrations of infectious virus, as determined by TCID50, were used to inoculate TZM-bl cells with increasing concentrations of RC-101 and ENF. Error bars represent SEM. Percent inhibition was calculated from RLU values and normalized to vehicle control (N=3-5). (**C+D**) The structure PDB 1IF3 was used to model the positions of primary gp41 mutations. HR1 (blue) mutations Q66R and V38A are shown along with nearby residues on HR2 (green) of the same gp41 molecule. Two additional gp41 molecules making up the 6-helix bundle are shown in gray.

The HR2 mutation N126K provides increased fitness in the presence of fusion inhibitors

To determine the effect of HR1 and HR2 mutations on viral replication, we subjected our mutants to 7-day viral fitness assays using lymphoblast-derived PM1 cells. Cells were infected in the presence of drugs or vehicle control using a relatively low titer (MOI 0.003). This ensured that the majority of infection would occur over a seven-day period, allowing us to determine the effects of each mutant on both drug resistance and on the overall replication fitness in culture.

In vehicle control conditions, virus containing the wild-type *env* consistently infected to a greater degree than the HR1-only mutants Q66R or V38A (**Figure 3**). In agreement with TZM-bl results, Q66R remained partially resistant to RC-101 at 5μg/ml, and completely susceptible to ENF. Oppositely, the V38A mutant was significantly inhibited by RC-101, yet remained resistant to ENF. When the HR2 mutation N126K was combined with Q66R, this double mutant no longer demonstrated significant replication differences from wild type virus in vehicle treated conditions, suggesting restored fitness. Furthermore, N126K imparted increased RC-101 and ENF resistance to the Q66R mutant. However, for the V38A mutant virus, N126K did not restore viral fitness in vehicle control conditions; instead, this double mutant suffered slightly reduced fitness compared to the V38A mutant virus ($p<0.05$). The secondary N126K mutation appeared to provide an increased ability to infect in the presence of ENF, though this trend was not statistically significant.

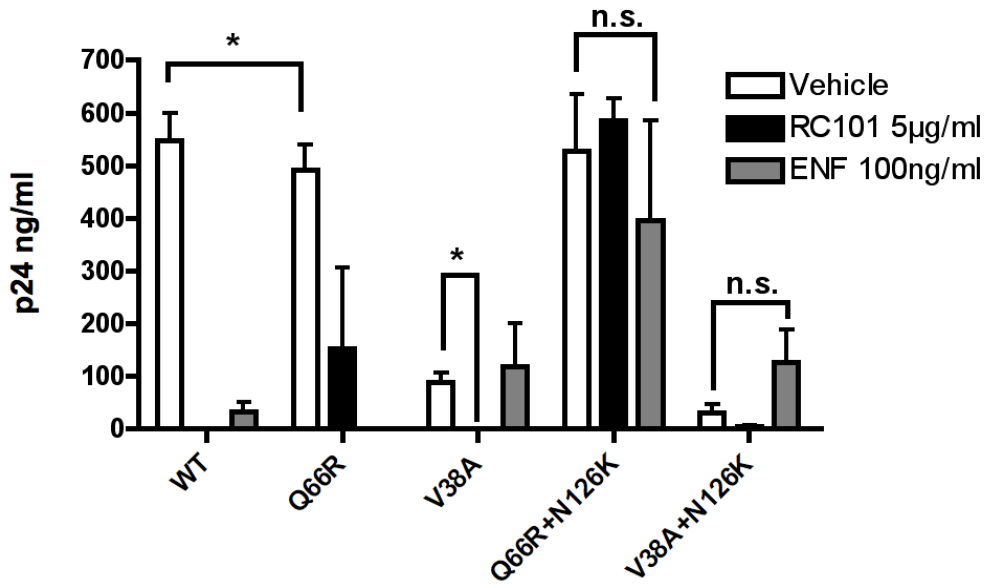

Figure 3: Analysis of Viral Fitness and Drug Resistance.

To determine if N126K is acting as a compensatory mutation in RC-101, viral fitness in culture over a 7 day period was determined for wild-type (WT) and drug-resistant mutants in the presence or absence of RC-101 and ENF. An MOI of 0.003, as determined by TCID50, was used for the initial inoculation of PM1 cells. Fitness was determined by p24 concentration measured in cell supernatants. Error bars represent SEM. Black lines indicate comparisons between conditions (N=3; *=p<0.05).

The effects of the N126K mutation in these experiments suggest that it acts as a compensatory mutation to restore viral fusion to the RC-101-resistant mutant Q66R. This observation suggests that N126K could be acting to increase the rate of gp41 fusion, potentially leading to a previously characterized hyperfusogenic phenotype observed during ENF resistance, but not understood to be implicated in RC-101 resistance [42].

N126K differentially enhances gp41 fusion efficiency compromised by drug-specific HR1 mutations

Our previous results suggest that the N126K mutation provides resistance to both fusion inhibitors tested. Based on this, we speculated that an increase in gp41 fusion efficiency could both restore fitness lost in the presence of inhibitors and provide resistance by fusing more rapidly, thus decreasing the possible time of interaction with fusion inhibitors. To observe potential differences in gp41 fusion between mutants, cell-cell fusion assays were performed. Cell-cell fusion was quantified by luciferase expression using target reporter TZM-bl cells following fusion with HIV Env- and Tat-expressing effector 293T cells. Cell-cell fusion was found to decrease by roughly half for both the Q66R and V38A HR1 mutants when compared with wild-type *env* (**Figure 4A and 4B**). Cells expressing N126K alone demonstrated a higher degree of fusion when compared with the wild-type *env*, while the Q66R+N126K combination restored fusion to roughly that of wild-type *env*. Interestingly, V38A+N126K displayed a 3.5-fold increase in fusion from wild-type, well beyond any of the other genotypes tested. In addition to data obtained by luciferase readings, imaging of GFP and *env* expressing cells revealed multinucleated fusion products whose sizes were proportional to cell-cell fusion as determined by luciferase readings and provided visual evidence comparing fusion between gp41 mutants (**Figure 4C**). Large syncytia were consistently more frequent in N126K- and V38A+N126K-expressing cells than with other genotypes. Conversely, effector cells expressing Q66R and V38A displayed numerous small, bright syncytia formed by relatively few cells. Together, these results reveal that the N126K mutation compensates for a loss of fusion due to either the Q66R or V38A primary mutations.

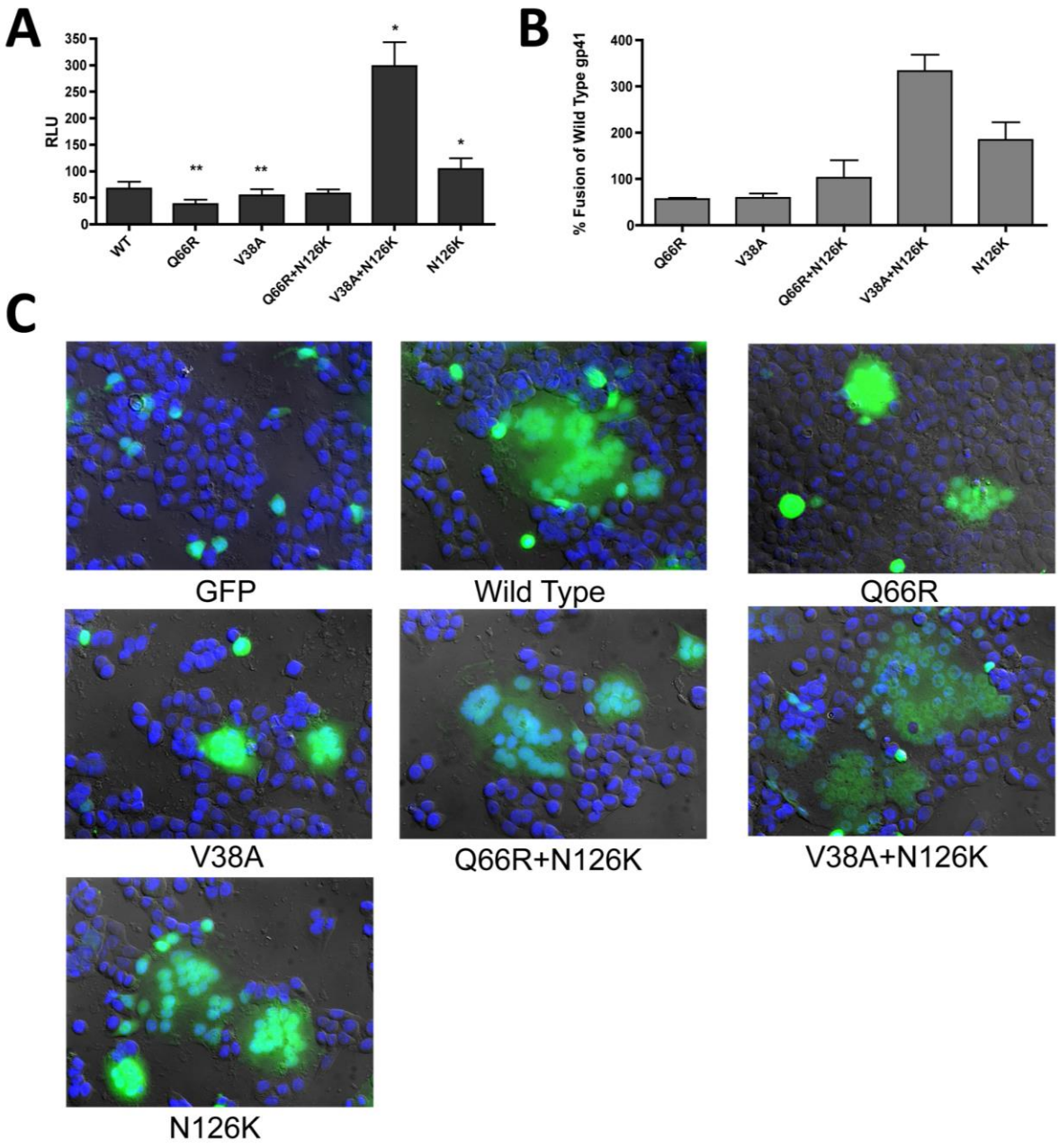

Figure 4: Effect of HR1 and HR2 Mutations on Cell-Cell Fusion.

Cell-cell fusion was analyzed to determine differences in gp41 fusion demonstrated by wild type (WT) and drug-resistant mutant virus. Transformed 293T cells expressing BaL Env and Tat proteins, as well as GFP, were co-cultured with TZM-bl reporter cells. (**A**) RLU values correlate with cell-cell fusion during co-culture, (**B**) which is also shown as percent fusion of WT. Error bars represent SEM. Fusion for each mutant virus was compared to that observed in WT (N=4; or 5 *=p<0.05, **=p<0.01). (**C**) Fluorescent imaging and DIC were used to observe syncytia formation as a secondary indicator to compare cell-cell fusion between mutants.

N126K restores viral entry kinetics compromised by Q66R

While our results demonstrate an increase in membrane fusion associated with the N126K mutation, we can only speculate as to how this may affect entry and possibly drug resistance. Previous studies suggest that a potential increase in the rate of gp41 fusion and entry is associated with drug resistance and can decrease the window of time when fusion inhibitors can act on the prefusion complex [42]. To determine if our RC-101-resistant mutants displayed differences in entry, we next investigated whether N126K could modify the rate at which our R5 molecular clones infected cells. Entry kinetics assays were carried out using equal amounts of infectious viral clones representing WT, Q66R, or Q66R+N126K *env* genotypes (**Figure 5**). There was a consistently sharp increase in infection by the WT and Q66R+N126K viruses at 30 minutes after transferring the cells from 4ºC to 37ºC to initiate infection. The Q66R single mutant virus demonstrated a significant lag in infection compared to both the WT and Q66R+N126K mutants at the points between 15 and 30 minutes. This experiment demonstrates that Q66R compromises the early stages of entry, and that N126K restores viral entry kinetics to levels observed in the WT.

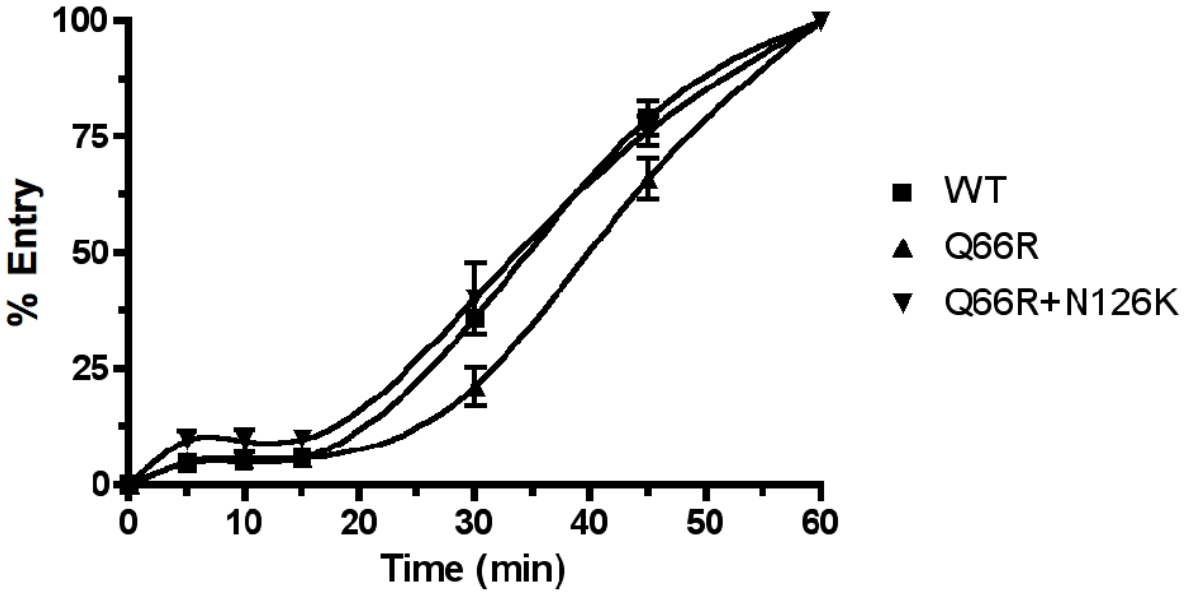

Figure 5: Entry Kinetics of RC-101 Resistant Virus

Viral entry was observed over one hour to determine differences in entry kinetics between wild type (WT) and RC-101-resistant virus. Equal concentrations of infectious virus were used to infect reporter cells and infection was halted at specific time-points. Entry kinetics is shown as percent of total entry and graphed using cubic splines. Linear regression curves were fit to data and slopes were compared between the 15 and 30-minute time intervals. Error bars represent SEM. Both wild type (WT) and Q66R+N126K had significantly greater slopes than the Q66R mutant (N=4; $p<0.05$).

N126K provides resistance to other structurally diverse peptide entry inhibitors

Our previous experiments indicate that the N126K mutation acts to restore fusion and rate of entry while providing RC-101 and ENF resistance. Since both RC-101 and ENF are thought to use different mechanisms for fusion inhibition, we hypothesized that this mutation would also provide resistance to other unique peptide entry inhibitors. Using the previously described TZM-bl viral inhibition assay, we infected cells with either wild-type, Q66R, or Q66R+N126K *env* mutants in the presence of RC107GG-F2, Grifonin-1, or the human α-defensin

HNP-1 at their reported EC50 concentrations. These peptides have all been identified as HIV-1 entry inhibitors and are believed to work through diverse mechanisms targeting the viral envelope [38,44,45]. Both Q66R and Q66R+N126K viruses displayed varying resistance to the antiviral peptides tested when compared to the wild-type virus (**Figure 6**). Alone, Q66R was able to provide resistance to both HNP-1 and Grifonin-1 at concentrations sufficient for inhibition of the wild-type virus, yet it remained susceptible to inhibition by RC107GG-F2. With the addition of N126K, we observed not only improved resistance to all peptides tested, but we saw increased infection in the presence of these peptides. These results demonstrate that the compensatory mutation N126K can provide improved resistance to a diverse set of peptides that act through inhibition of viral entry.

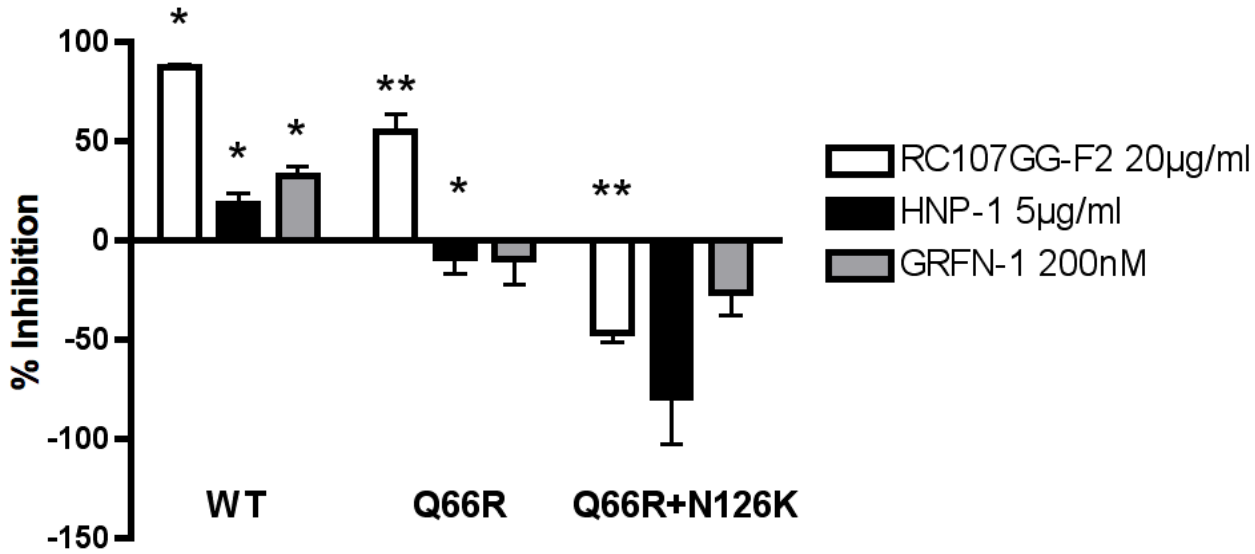

Figure 6: Resistance to Alternative Peptide Entry Inhibitors in RC-101-Resistant Virus

Susceptibility to antiviral peptides in wild type (WT) and RC-101-resistant mutants was determined using infection TZM-bl reporter cells. The antiviral peptides RC107GG-F2, HNP-1, and Grifonin-1 (GRFN-1) were used at concentrations known to inhibit infection by wild type virus. Percent inhibition of infection was calculated from RLU values and normalized to vehicle controls. Error bars represent SEM. Percent inhibition values were compared with infection using vehicle control alone (N=3; *=p<0.05, **=p<0.01).

Discussion

We observed that while single HR1 mutations provide some degree of drug resistance, this resistance is specific for either RC-101 or ENF. The V38A substitution, in particular, has been shown to be associated with resistance against multiple C-peptide type fusion inhibitors, yet we found V38A mutants remained susceptible to inhibition by RC-101. This is likely due to different gp41-binding regions for the two drugs, as ENF aligns with its corresponding HR1 residues closer to the N-terminus of gp41 and RC-101 is known to bind to HR2 [46]. The V38A single mutant remaining susceptible to RC-101 provides evidence that RC-101 targets a region outside of the ENF binding site. This finding is particularly promising since RC-101, and similarly acting θ-defensins, would likely remain active against HIV-1 harboring other ENF-resistance mutations such as those frequently observed in the "GIV" region of HR1 [47,48].

Irrespective of the specificity of either HR1 mutation, N126K provided some degree of resistance to both drugs despite the clear differences in not only the structure of both inhibitors tested, but also the different binding sites of these peptides on gp41. Moreover, we have shown that N126K has a different effect on fusion depending on the primary mutation present in HR1 responsible for providing drug resistance. The effect on fusion associated with Q66R and V38A may again be explained by their similar locations on the HR1 helix. Both Q66R and V38A occupy the same position of the helical turn directly interacting with the HR2 helix of the same molecule and could reasonably affect membrane fusion in a similar way. The comparable effect on fusion seen with HR1 mutations is contrasted by the difference in compensatory activity with the addition of N126K. While the V38A+N126K genotype appears to overcompensate for the loss of fusion associated with V38A, Q66R+N126K restores fusion to

the level of the wild-type virus. This observation may explain differences in fitness in the absence of fusion inhibitors displayed by the two double-mutants. Previous studies have demonstrated that N126K leads to a rapidly fusing gp41 that is dependent on ENF for infection. However, with our Q66R+N126K mutant we observed that fitness was not affected and that fusion and entry kinetics were restored to the levels of the wild-type virus. This observation is perhaps due to the differences in how Q66R or V38A would affect the formation of the mature gp41 complex. The difference being, that while V38A merely exchanges one small hydrophobic residue for another, perhaps reducing HR1's affinity for both HR2 and ENF, Q66R inserts a large cationic residue into the hydrophobic pocket of gp41 that could not only act to repel a cationic peptide such as RC-101, but would also sterically constrain two key tryptophan residues located in the corresponding region of HR2 that are believed to play a significant role in the activity of gp41 [28]. This key difference may explain why we see overcompensation in fusion observed with V38A+N126K, while Q66R+N126K only exhibits restored fusion when compared with the wild type.

One question that remained was how N126K could provide increased resistance to RC-101 when it merely restored gp41 activity to that observed in the wild type. It is reasonable to assume that if N126K was in fact increasing fusion beyond what is seen in the wild-type virus, then the time in which gp41 is exposed to fusion inhibitors would decrease, and thus the kinetic window wherein fusion inhibitors exert their activity would be reduced as well. However, N126K only increased fusion when compared to Q66R alone, thus still decreasing the time that RC-101 could interact with gp41 while maintaining the resistance imparted by Q66R. This would

explain the increase in RC-101 resistance as corresponding to a decrease in the time available for RC-101 to exert its activity.

A remaining question is why partial ENF resistance was achieved with the Q66R+N126K virus when N126K appears to only restore gp41 activity to that of the ENF-susceptible wild-type virus. Interestingly, Q66R has been identified in a patient receiving ENF treatment and may have been selected for by treatment [49]. In contrast, our experiments show that Q66R alone was not sufficient to provide any noticeable ENF resistance. This difference is possibly due to our studies utilizing the *env* derived from an R5 virus, rather than the more frequently studied X4 strains, which are known to display differences in entry rates, possibly due to utilization of separate coreceptors [50].

We have shown here that the same evolutionary path could achieve resistance to two distinctly different fusion inhibitors. Further, we have described the contribution of a secondary mutation responsible for the observed cross-resistance while exploring the mechanism by which resistance could be achieved. These findings were then applied to demonstrate how this mutation could provide improved resistance to other unique peptide entry inhibitors. Additionally, we show for the first time that RC-101 can inhibit the clinically significant enfuvirtide-resistant mutants V38A and V38+N126K. This insight provides us with direction in the continued development of fusion inhibitors and underscores the importance of compensatory HR2 mutations in drug-resistance.

CHAPTER 3: COMBINATION FUSION AND REVERSE TRANSCRIPTASE INHIBITORS PROVIDE ROBUST PROTECTION AGAINST DIVERSE HIV ISOLATES

Introduction

Inconsistent drug susceptibility due to genetic variability within HIV-1 presents a major hurdle in microbicide development [51-53]. While these mutations are often the result of selection during antiretroviral treatment, naturally occurring mutations across viral subtypes can also contribute to the difficulty in finding specific, mechanism-based antivirals which can remain effective when formulated into microbicides. This is further complicated by the high degree of genetic diversity in HIV in Sub-Saharan Africa, where microbicides offer the most promise [54]. A possible solution to this is the formulation of microbicides consisting of two or more mechanistically distinct antiretroviral drugs.

Drug-resistance mutations, whether naturally occurring or resulting from selection during treatment, often provide resistance to several drugs within a particular class defined by the mechanism of inhibition. One such example is the HIV-1 gp41 mutation V38A, which not only provides resistance to the fusion inhibitor enfuvirtide, but also to second and third generation peptide fusion inhibitors [34,47,55]. This issue of cross-resistance also presents a problem for several of the non-nucleotide reverse transcriptase inhibitors (NNRTI) in development. The RT mutations K103N and L100I, provide resistance to a variety of NNRTI drugs such as Etravirine, Rilpivirine, and Efavirenz [53].

Here we determined the activity of a peptide fusion inhibitor, RC-101, and an NNRTI, 5-chloro-3-phenylsulfonylindole-2-carboxamide (CSIC), against diverse HIV-1 clinical isolates from

five Group M subtypes. We then tested the activity of CSIC and RC-101 against virus with mutations providing either partial RC-101 or CSIC resistance. We found that CSIC and RC-101 naïve clinical isolates possessed variable susceptibility to RC-101 and CSIC, with some isolates showing naturally decreased inhibition by either RC-101 or CSIC. We also observed that CSIC maintained antiviral activity against virus containing the known RC-101 resistance mutations Q66R and Q66R+N126K. RC-101 also maintained antiviral activity against virus containing the NNRTI resistant genotype K103N + L100I. These experiments suggest that a combination approach using RC-101 and CSIC in a single microbicide formulation could provide robust protection against a variety of genetic backgrounds in HIV-1.

Materials and Methods

Cell Lines and HIV-1 Strains

TZM-bl luciferase reporter cells were obtained from the NIH AIDS Research and Reference Reagent Program, Division of AIDS, NIAID, NIH from Dr. J.C. Kappes (University of Alabama, Birmingham, AL) and Dr. X. Wu (University of Alabama, Birmingham, AL and Tranzyme, Research Triangle, NC). TZM-bl cells were maintained in DMEM supplemented with 10% fetal bovine serum with penicillin and streptomycin. Cells were stored at 37 °C and 5% CO_2.

Several clinical isolates representing the three most prevalent HIV subtypes, A, B, and C were used to determine differences in antiviral activity. HIV-1 isolates 94UG114, 92UG037, 92US712, 93MW960, 92RW008, 92UG029, 93UG070, 93UG067, 93BR020 were obtained from

the NIH AIDS Research and Reference Reagent Program, Division of AIDS, NIAID, NIH. The pBaL molecular clone was constructed as described previously [56].

Antiviral Drugs

The 18 amino acid RC-101 peptide was synthesized as previously described [29,36]. RC-101 was resuspended in molecular grade water with 0.01% acetic acid at 1 mg/mL concentration. CSIC was provided by Dr. Michael Parniak at the University of Pittsburgh. CSIC stocks were prepared in DMSO and stored at 10 mM concentrations.

Antiviral Activity Assays

TZM-bl luciferase reporter cells were used to determine inhibition of infection as previously described [29]. TZM-bl cells were plated in 96-well, black, transparent bottomed plates at a density of 5×10^4 cells per well in 100 µL of the previously described culture media. 24 hours after plating, media was removed and replaced with peptide or vehicle control in 50 µL culture media before incubation for 10 minutes at 37 ºC and 5% CO_2. HIV-1 representing the indicated strains was added to cells at equivalent concentrations of infectious particles (as determined by RLU in TZM-bl cells). Virus was premixed with or without DEAE dextran prior to infection as indicated.

Results and Discussion

To evaluate susceptibility across a range of diverse HIV-1 subtypes, RC-101 and CSIC (Figure 7**A and 7B**) were used to treat TZM-bl cells prior to infection with the indicated HIV-1 strains (Table 1).

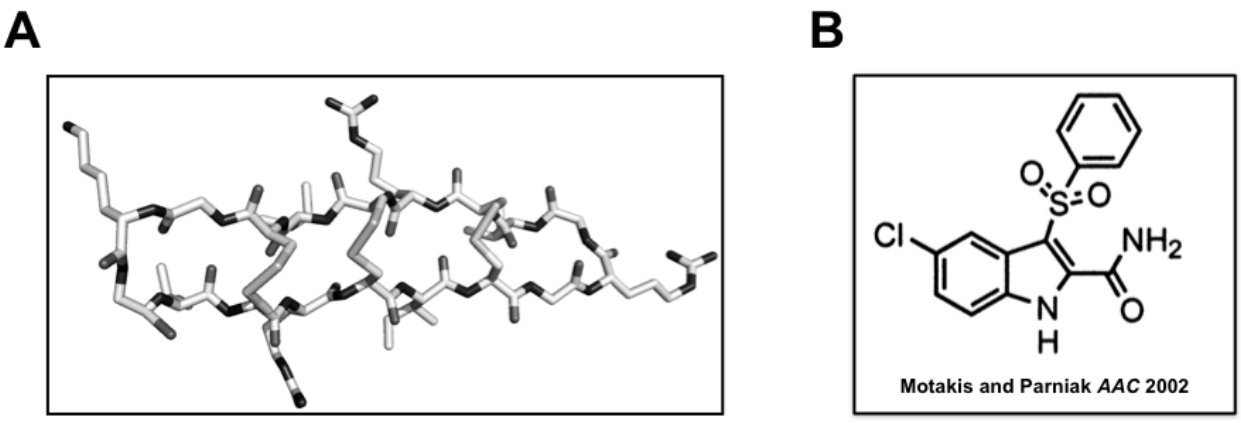

Figure 7: Structures of antiviral compounds RC-101 and CSIC

The structures of two antiviral molecules are shown above. (**A**) The fusion inhibitor RC-101 is a cyclic, 18 amino acid peptide containing three disulfide bonds. (**B**) The NNRTI CSIC is a small molecule that acts by binding tightly to HIV-1 RT.

Table 1: Lab-adapted strains and clinical isolates of HIV-1

Strain/Isolate	Tropism	Subtype
pNBaL	R5	B
92UG037	R5	A
92RW008	R5	A
92UG029	X4	A
91US005	R5	B
92US712	R5	B
93MW960	R5	C
93UG070	X4	D
93UG067	R5X4	D
94UG114	R5	D
93BR020	R5X4	F
33015	R5	–
33074	X4	–

At 3 µM, the activity RC-101 ranged from 12.3% inhibition (93MW960) to 81.7% inhibition (33015) (**Figure 8A**). This result is consistent with previous findings demonstrating decreased susceptibility to RC-101 in some subtype C strains [20]. At 0.5 nM, the activity of CSIC ranged from 33.6% inhibition (92UG029) to 94.1% inhibition (33015). Since some clinical strains required unusually high volumes of inoculum to achieve infection, experiments were repeated premixing virus with DEAE dextran to aid in cell attachment and allow for more uniform inoculation volumes (**Figure 8B and 8C**). These experiments were also carried out using a range of 5 concentrations for both RC-101 and CSIC. After generating dose response curves, we found that RC-101 had EC50 values ranging from 1.25 µM (92UG037) to 4 µM (93MW960). CSIC had EC50 values ranging from 4 nM (92UG037) to 8.5 nM (93RW008). These experiments demonstrate that, even within the limited pool of clinical isolates tested, some strains will be naturally less susceptible to either drug. This evidence highlights the importance of combining two broad spectrum antiretrovirals like RC-101 and CSIC in a single microbicide.

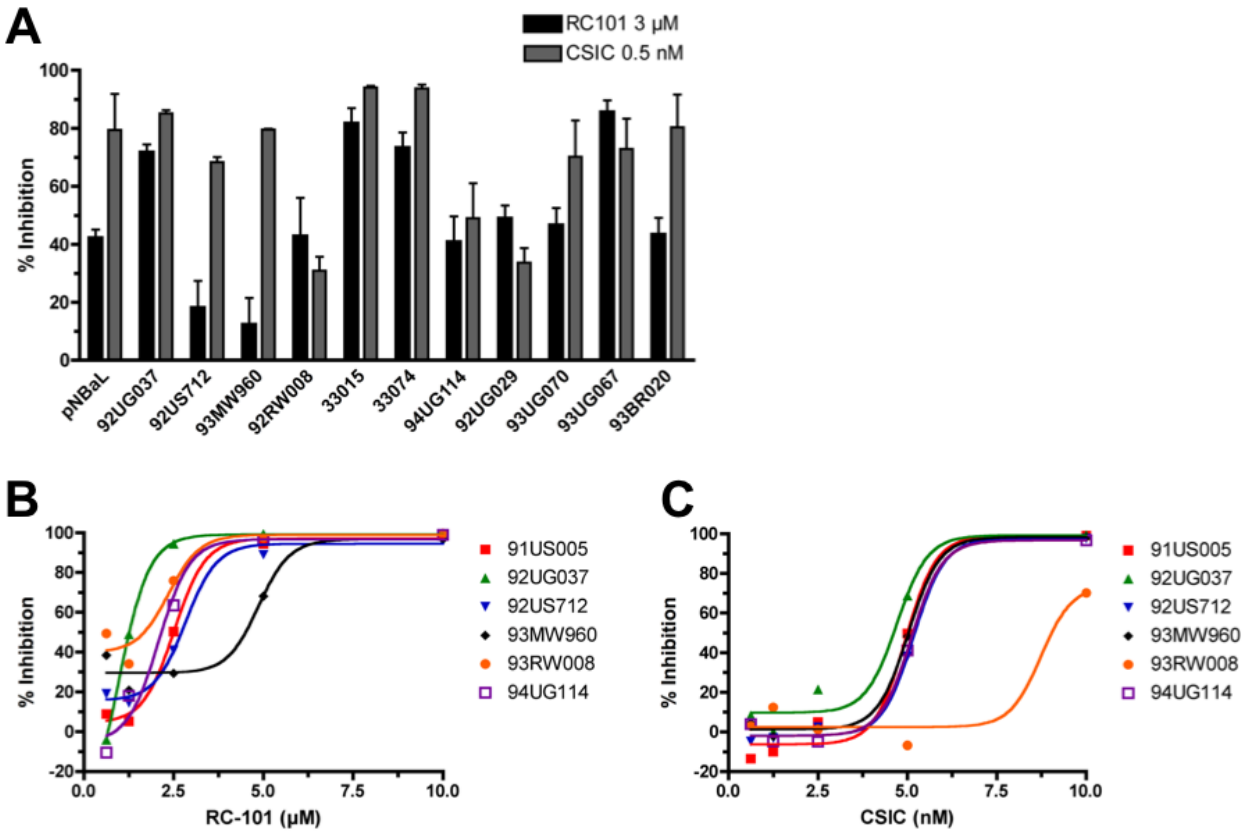

Figure 8: Genetically diverse clinical isolates possess varying susceptibility to RC-101 and CSIC.

(**A**) The pNBaL molecular clone, along with clinical isolates representing five HIV-1 subtypes, were used to infect TZM-bl reporter cells in the presence of 3 µM RC-101, 0.5 nM CSIC, or a corresponding vehicle control. Error bars represent SEM (N=3). Clinical isolates were used to infect TZM-bl reporter cells at the indicated concentrations of (**B**) RC-101 or (**C**) CSIC. Curves were generated using nonlinear regression.

We next examined susceptibility of drug-resistant virus to either RC-101 or CSIC. We first tested CSIC at indicated concentrations against previously identified partial RC-101-resistant genotypes Q66R and Q66R+N126K (**Figure 9A and 9B**). We also used the RCres virus containing several mutations, including Q66R and N126K, which developed after prolonged passaging of the BaL strain with sub-inhibitory concentrations of RC-101 [29]. At 0.1 nM, CSIC was able to inhibit infection of TZM-bl cells by roughly 50% for both the wild type BaL and mutant viruses, while 1 nM completely inhibited infection for all viruses. This result

demonstrates that CSIC would not be affected by specific mutations providing resistance to RC-101.

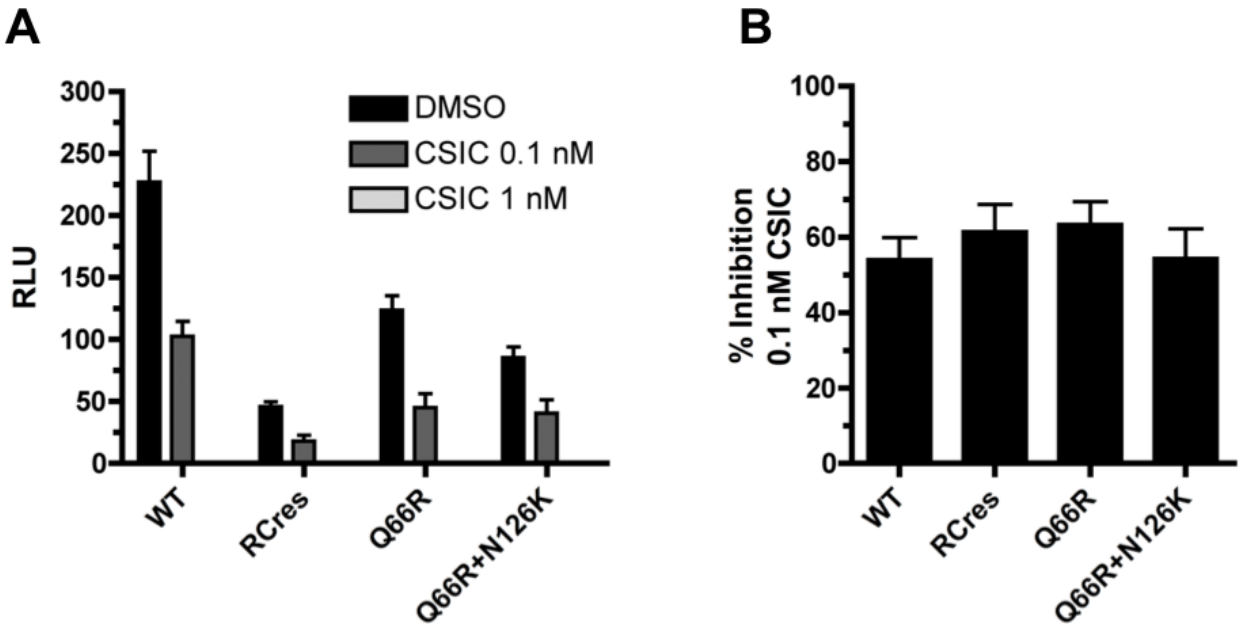

Figure 9: Mutations providing resistance to RC-101 do not affect susceptibility to CSIC.

Wild-type (WT), RC-101 passaged Env (RCres), and RC-101 resistant genotypes Q66R and Q66R+N126K were used to infect TZM-bl reporter cells. (**A**) Relative light unit values are reported for infections with four virus genotypes in the presence of a DMSO (vehicle) control or CSIC at the indicated concentrations. (**B**) The percent inhibition of infection is shown for the same viruses using CSIC at 0.1 nM. Error bars represent SEM (N=3).

Tight-binding NNRTI's, such as CSIC and Efavirenz offer the potential for development into microbicides due to their improved binding kinetics over earlier generation NNRTIs [57]. To further determine the benefits of an RC-101 and CSIC combination, the activity of both drugs was evaluated using both wild type HIV-1 and the NNRTI-resistant L100I+K103N genotype (**Figure 10**). In addition to being tested individually, RC-101 and CSIC were combined at a 1:1 molar ratio at the indicated concentrations. The combination index (CI) was then calculated to determine if RC-101+CSIC had either and additive or synergistic effect. While for wild type virus

the CI of 1.2 suggested additive activity, the activity against L100I+K103N showed a CI of 0.5, thereby demonstrating the synergistic activity of RC-101+CSIC.

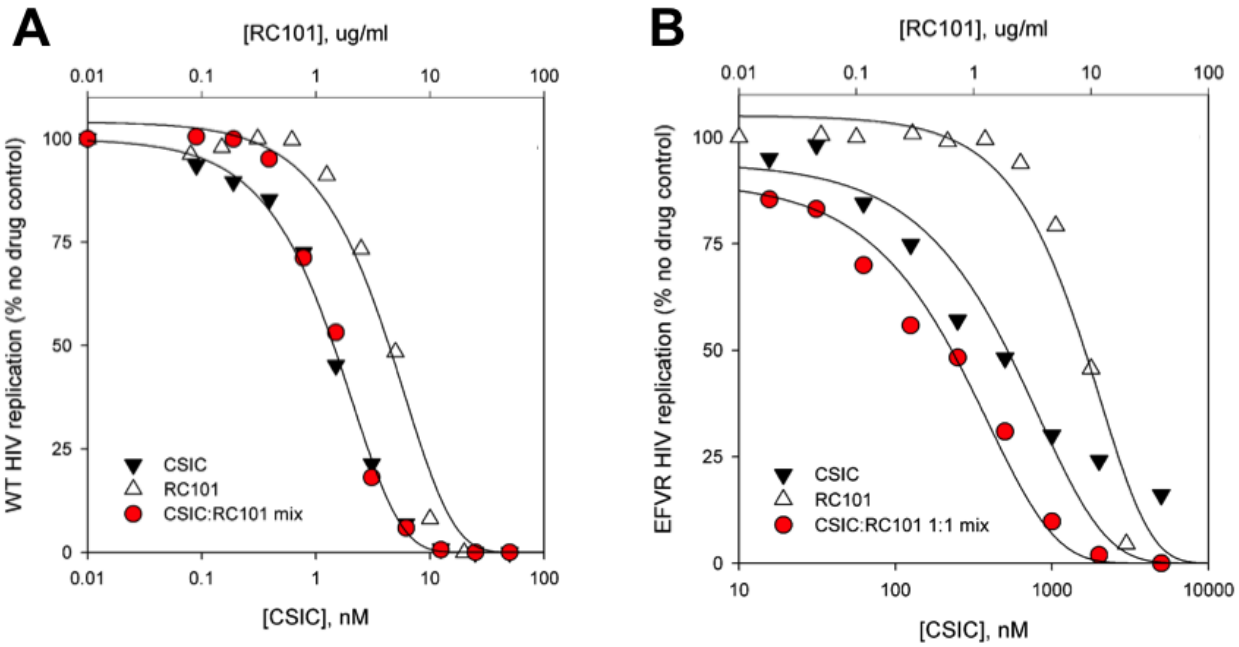

Figure 10: RC-101 confers synergistic with CSIC against NNRTI-resistant HIV-1

Dose response curves were generated for (**A**) CSIC + RC-101 against wild type HIV-1 and (**B**) CSIC + RC-101 against the NNRTI-resistant L100I+K103N mutant. The combination index at EC_{90} was calculated to determine if results were additive or synergistic. Figure provided by the laboratory of Dr. Michael Parniak.

The activity of RC-101 and CSIC against clinical isolates was complementary. Importantly, RC101 was effective against clinical isolates that were less susceptible to CSIC, and vice versa, suggesting that the combination would increase the spectrum of susceptible isolates. RC-101 was fully active against virus containing the clinically significant NNRTI resistance mutations L100I+K103N. CSIC could completely inhibit mutants possessing partial resistance to RC-101.

These findings imply the potential efficacy of using RC-101 with CSIC in a microbicide to counter genetically diverse virus populations. The activity of CSIC is not compromised by

mutations providing partial resistance to fusion inhibitors. The compensatory effect of combining these two mechanistically distinct drugs would overcome partial resistance afforded by the natural variation in gp41 and reverse transcriptase. In this way, developing microbicides employing RC-101 and CSIC could offer protection against a broad range of clinically occurring viruses.

CHAPTER 4: THE HIV GP41 ECTODOMAIN IS CLEAVED BY MATRIPTASE TO PRODUCE A CHEMOTACTIC PEPTIDE THAT ACTS THROUGH FPR2

Introduction

The envelope of HIV-1 is coated in glycoproteins, gp120 and gp41, that enable the virus to bind, fuse, and infect susceptible host cells. In addition to mediating viral fusion, gp41 has been implicated in immunosuppressive cytokine production and induction of apoptosis [58-60]. Additionally, synthetic peptides derived from gp41 have been shown to be chemotactic agonists through the formyl peptide receptor FPR2 [61-63]. Despite exhibiting chemotactic properties that could affect transmission and virulence, no study has reported how these peptides could be naturally produced within the host.

The ectodomain of gp41 on the surface of the viral envelope consists predominantly of the helical heptad repeats 1 and 2 (HR1 and HR2), which are joined by a disulfide loop. HR1 is exposed to the extracellular environment, and a large number of antibodies are known to target the gp41 immunodominant domain located at the C-terminal region of HR1 at gp41 residues 68-102 [64,65]. This stretch of amino acids is unusually conserved and overlaps with areas of gp41 exhibiting activity other than membrane fusion [66,67]. This region of gp41 is therefore of particular interest as a potential site for proteolytic digestion, which could produce peptides independent from the intact virion. These peptides may then induce chemotaxis of susceptible host cells for infection.

During infection, the majority of HIV-1 resides in host tissue reservoirs where the virus may replicate while evading antiviral immunity [68,69]. One such reservoir is the prostate,

where epithelial cells efficiently bind, and transfer HIV to target CCR5-expressing leukocytes [66,67]. The prostate is also an important viral reservoir in terms of the dissemination of HIV, with semen being the most predominant vehicle of transmission. Within the prostate, a number of well-characterized serine proteases exist on the surface of epithelial cells or within prostatic fluid. This environment therefore represents an area where proteolytic maturation of immunomodulatory gp41 peptides likely occurs. Synthetic HR1 peptides can be produced to represent a region of the gp41 ectodomain that would be exposed to the extracellular environment, including proteases found on the apical membranes of epithelial cells [70]. In this study we determined if an HR1-derived peptide could be cleaved by prostatic epithelial proteases into chemotaxis-inducing peptides that function through FPR2.

By examining overlapping peptides of gp41 HR1, we identified a 7-residue region of HR1 that was associated with chemotactic activity toward HL-60 neutrophils. We then evaluated the proteolytic activity of several epithelial proteases found in the prostate against an HR1 peptide using in vitro digestion assays. We determined that matriptase efficiently cleaves a region of gp41 at biochemically-conserved matriptase-recognition sites located within the leucine zipper motif. A 22-residue peptide cleavage product, MAT-1, was identified and found to exhibit chemotactic activity in HL-60 neutrophils and primary monocytes. We then demonstrated that expression of the receptor FPR2 mediated the observed chemotaxis in response to MAT-1. This work demonstrates a potential mechanism by which chemotactic peptides can be produced within the host, during infection with HIV-1.

Materials and Methods

Peptides and DNA Constructs

The 15-mer peptide set corresponding to the HIV-1 subtype B (MN) envelope was obtained from the NIH AIDS Research Reagent Program (Division of AIDS, NIAID, NIH). Synthetic peptides were generated using solid phase synthesis. T21, PAP286, and MAT-1 were custom synthesized by Peptide 2.0, (Chantilly, VA). LL-37 and the peptide negative control RREQALLIYVA were synthesized by Bachem (Torrance, CA). Peptides were purified to >99% purity by HPLC and verified by mass spectrometry. WRW4 and WKYMVm were purchased from Anaspec (Fremont, CA). fMLP was purchased from Sigma Aldrich (St. Louis, M). Cyclosporin H was purchased from Santa Cruz Biotechnology (Santa Cruz, CA).

The FPR2 gene was cloned from human monocyte cDNA using the primers FPR2_S: ATGGAAACCAACTTCTCCACTCCTCTGAAT and FPR2_AS: TCACATTGCCTGTAACTCAGTCTCTGCAGG. PCR amplicons were purified and inserted into the TOPO-TA cloning vector before being digested with EcoR1 and subcloned into the mammalian expression vector pcDNA3 (Life Technologies, Carlsbad, CA). Sequences were confirmed by Sanger sequencing using FPR2 and pcDNA-specific primers FPR2_AS and T7, respectively.

Primary and Immortalized Cells

The HL-60 cell line was purchased from the American Type Culture Collection (ATCC) and was maintained in RPMI 1640 with penicillin, streptomycin, 10 mM HEPES, and 20% fetal bovine serum (R20). For chemotaxis assays, HL-60 cells were differentiated into neutrophil-like

cells as previously described [71,72]. Briefly, cells were resuspended in R20 with 1.3% DMSO at 2.0 × 105 cells/mL and allowed to proliferate and differentiate into neutrophils for 6 days. Differentiation was verified morphologically using Diff-Quik stain (Dade Behring Inc., Newark, DE) with bright-field microscopy. Neutrophils were used within 3 days after differentiation. HEK 293 cells were purchased from ATCC and maintained in Dulbecco's Modified Eagle Media (DMEM) supplemented with penicillin, streptomycin, 10 mM HEPES, and 10% fetal bovine serum. HEK 293 cells were transfected with either the pcDNA3/FPR2 construct described above or the pcDNA3 vector alone using the Effectene transfection system (QIAGEN, Hilden, DE). Stable FPR2-expressing cells were selected by passaging cells in the presence of 1.5 mg/mL G418 for 30 days. Expression of FPR2 was confirmed by RT-PCR, western blot and flow cytometry as described below.

To obtain primary cells, blood was drawn from healthy donors following informed consent with approval from the Institutional Review Board at the University of Central Florida. Blood was collected in acid-citrate-dextrose and divided for isolation of monocytes or neutrophils. For monocyte purification by negative selection gradient centrifugation with the RosetteSepTM Human Monocyte Enrichment Cocktail (Stem Cell Technologies, Grenoble, France) and Ficoll-PaqueTM PLUS (GE Healthcare) was performed following the manufacturers instructions. This system utilizes tetrameric antibody complexes to achieve negative selection of monocytes. Briefly, 750 µl of antibody reagent was combined with 15 ml of whole blood and allowed to incubate for 20 minutes at room temperature. The blood was then diluted with an additional 15 ml of PBS + 2% FBS and 1 mM EDTA and layered onto 15 ml of Ficoll-Paque PLUS gradient. Blood was centrifuged at 1200 × g for 20 minutes at room temperature. Enriched cells

were harvested and washed twice with PBS + 2% FBS. Monocyte purification by positive selection was carried out using cell-sorting methods. Monocytes were labeled with phycoerythrin-conjugated anti-CD14 antibody reagent (Becton-Dickinson, Franklin Lakes, NJ) at 100 µL for 1.0 × 107 cells at 1.0 × 106 cells/mL PBMC for 30 minutes at room temperature in HBSS with 1% FBS. CD14 positive monocytes were sorted (BD FACSJazz; Becton-Dickinson) and maintained in RPMI 1640 with penicillin, streptomycin, 10 mM HEPES, and 10% fetal bovine serum prior to use in chemotaxis experiments. For primary neutrophil isolation, whole blood was treated with erythrocyte lysis buffer (150 mM NaCl, 10 mM NaHCO3, and 1.3 mM EDTA) at a 10:1 ratio of lysis buffer to blood. After 3-5 minutes lysis buffer was immediately neutralized using an equal volume of HBSS. Cells were washed twice in HBSS and resuspended in HBSS with 1% FBS and then isolated by using forward scatter and side scatter (BD FACSJazz) to identify and sort neutrophils.

Chemotaxis Assays

Chemotaxis was determined using a 48-well microchemotaxis chamber (Neuro Probe, Cabin John, MA). Peptides were diluted in chemotaxis media (RPMI 1640 with penicillin/streptomycin, 10 mM HEPES, and 1% bovine serum albumin) and pre-warmed at 37 ºC before being added to the lower compartment of the chemotaxis chamber. Polycarbonate filters were then positioned over the lower compartments before assembling the complete chamber. For HL-60 neutrophils, primary monocytes, and HEK 293 cells, filters containing 5 µm pores were used. For primary neutrophils, filters with 3 µm pores were used. For monocyte chemotaxis, filters were purchased pre-coated with poly-vinyl-pyrollidone. For HEK 293

chemotaxis, filters were coated for 2 hours in 0.05% type-1 rat tail collagen (BD Biosciences, Bedford, MA) in RPMI 1640 with 70 mM HEPES. Prior to chemotaxis, cells were washed once in phosphate buffered saline (PBS), resuspended in chemotaxis media (5.0 × 105 cells/mL for HL-60 neutrophils and 1.0 × 106 cells/mL for primary monocytes, primary neutrophils and HEK 293 cells), and applied to the upper compartment of the chamber. The microchemotaxis chamber was then incubated for 1 hour (neutrophils and monocytes) or 5 hours (HEK 293 cells) at 37 ºC and 5% CO2. Filters were scraped to remove cells that did not migrate and fixed in methanol for 1 minute. Filters were stained using Diff-Quik (Dade Behring Inc.) and mounted to glass slides with coverslips for imaging. Cells from five high-powered fields (400X) were quantified using the FIJI package of ImageJ software and averaged for each repeat. The chemotaxis index (CI) was calculated for each condition as the fold-increase in migrated cells versus media.

Analysis of FPR2 Expression

FPR2 specific primers for real-time RT-PCR were designed using Beacon Design software version 7.5. The following primer pairs were used for RT-PCR, S: CACATTACCATTCCTCAT and AS: AACCAATCAAGAAGACAC for FPR2 and S: TGGTATCGTGGAAGGACTC and AS: AGTAGAGGCAGGGATGATG for GAPDH. HEK 293 cells transfected with pcDNA3, pcDNA3/FPR2, or untransfected cells were grown to confluency in 6-well plates. After removal of media, cells were washed once with PBS and treated with 0.5 mL of TRIzol Reagent (Life Technologies) following the manufacturer's instructions. After isolation of RNA, cDNA was produced by incubation with reverse transcriptase using the iScript system (Bio-Rad). Each 20 µL reaction contained 1 µg of template RNA. Relative levels of cDNA were measured using the SYBR Green

RT-PCR Reagents Kit (Bio-Rad). Briefly, FPR2 and GAPDH cDNA were amplified using 1 cycle of melting at 95 ºC for 5 minutes followed by 40 cycles of amplification with annealing and extension at 55.7 ºC. Melt curve analysis confirmed the absence of non-specific products and curve fit RFU values were baseline subtracted. Cycle thresholds were normalized to GAPDH and fold-expression was calculated using the ΔΔCT method [73].

For confirmation of FPR2 protein expression, HEK 293 cells were grown to confluency in 6-well plates and lysed to isolate membrane fractions as shown previously [74]. Protein concentrations were determined using the DC Protein Assay (Bio-Rad) with a BSA standard curve. For each cell type, 15 µg of total protein were resolved on pre-cast 4-20% gradient polyacrylamide gels (Thermo-Fisher Pierce Protein Biology Products, Rockford, IL). Proteins were transferred to PVDF membranes and blotted for FPR2 using rabbit polyclonal anti-FPR2 (ab63022, Abcam, Cambridge, ENG) following an established western blot protocol [75]. PVDF membranes were blotted using secondary goat anti-rabbit HRP-conjugated antibodies and developed using Protein Simple chemiluminescent substrate (GE Healthcare, Little Chalfont, UK). Developed membranes were visualized with a Chemi-Doc imaging system (Bio-Rad, Hercules, CA.)

FPR2 expression in HEK 293 cells was determined using a FACSJazz flow cytometer. Phycoerythrin-conjugated anti-FPR2 antibody (Santa Cruz Biotechnology, Santa Cruz, CA) was incubated with cells for 30 minutes at room temperature in Hank's Balanced Salt Solution (HBSS) with 1% FBS. A 2 mL suspension of HEK 293 cells at 1.0 × 106 cells/mL was labeled following the manufacturers instructions at 1 µg of antibody/1.0 × 106 cells. Analysis was performed using FlowJo Version X software.

Identification of Proteolytic Cleavage Products

Prostate-specific antigen (PSA)/KLK3 purified from human semen was obtained commercially (Sigma Aldrich, St. Louis, MO). Recombinant prostasin was purified as described previously [76] and matriptase was obtained commercially (R&D systems, Minneapolis, MN). All peptide digestions were prepared in Dulbecco's Modified Phosphate Buffered Saline (DPBS). T21 and PAP286 peptides were used at 50 µM concentrations. Prostasin and matriptase were used at final concentrations of 2 nM and 1 nM, respectively. PSA was used at 50 nM as previously described [77]. Digestions were carried out in 10 µL reactions in DPBS and incubated for 24 hours at 37 ºC, shaking at 300 rpm. Digestion products were electrophoresed on Tricine-SDS 16% polyacrylamide gels for 3 hours at 70V. The remaining digestion products were brought to 50% acetonitrile (ACN) and 0.1% trifluoroacetic acid (TFA) before mixing 1:1 with 10 mg/mL alpha-Cyano-4-hydroxycinnamic acid matrix dissolved in 50% ACN and 0.1% TFA. Samples were analyzed by MALDI-TOF MS on a Microflex mass spectrometer (Bruker Daltonics, Billerica, MA, USA) in positive reflectron mode. External calibration was performed using a peptide-range mass standards kit (Bruker Daltonics). Mass spectra results were analyzed using Flex Analysis software (Bruker Daltonics).

Protein and DNA Sequence Analysis

HIV and SIV Env sequences were obtained from the 2012 HIV Sequence Compendium (Los Alamos National Laboratory). Representative protein alignments were prepared using the MUSCLE multiple sequence alignment software in MEGA version 5 [78]. Shannon Entropy for Group M Subtype B sequences was calculated using the Entropy-One tool provided by the HIV

Sequence Database (Los Alamos National Laboratory): http://www.hiv.lanl.gov/content/sequence/ENTROPY/entropy_one.html. DNA alignments were prepared from representative gp41 ectodomain sequences from diverse HIV clades. Maximum Likelihood trees with bootstrapping were generated from alignments using MEGA version 5.

Statistical Analysis

Chemotactic activity for each peptide in the initial HR1 screen was compared to the media control using the Student's T-test. For experiments with multiple peptide concentrations, a two-way ANOVA with Bonferroni post tests was used to compare every concentration of unknown or positive control to its corresponding equal concentration of negative control peptide. D'agostino normality and Mann-Whitney U tests were used to analyze nonparametric median Shannon Entropy data.

Results

Chemotactic activity of gp41 HR1 is localized to two distinct regions

To determine the regions of gp41 HR1 associated with chemotaxis, overlapping 15-mer peptides derived from HIV LAI HR1 were individually tested for chemotactic activity in HL-60-derived neutrophils. These cells have been shown in earlier studies to express FPR2 [79,80], a receptor previously implicated in the chemotactic activity of gp41 [62,63], which we confirmed (not shown). Of the 16 HR1 peptides we tested, 6342–6346 and 6351–6353 were shown to significantly induce chemotaxis, exhibiting 2-3-fold greater activity than the vehicle control

(**Figure 11Aand 11B**). The peptide WKYMVm was used as a positive control for HL-60 neutrophil chemotaxis through FPR2 [81]. The region of HR1 represented by peptides 6351–6353 overlaps with the synthetic peptide T21/DP-107 (**Figure 11C**). T21 has been previously characterized as a chemotactic peptide for primary monocytes and neutrophils 6. Peptides 6351–6353 also share the LQARVLA sequence, which potentially imparts chemotactic activity.

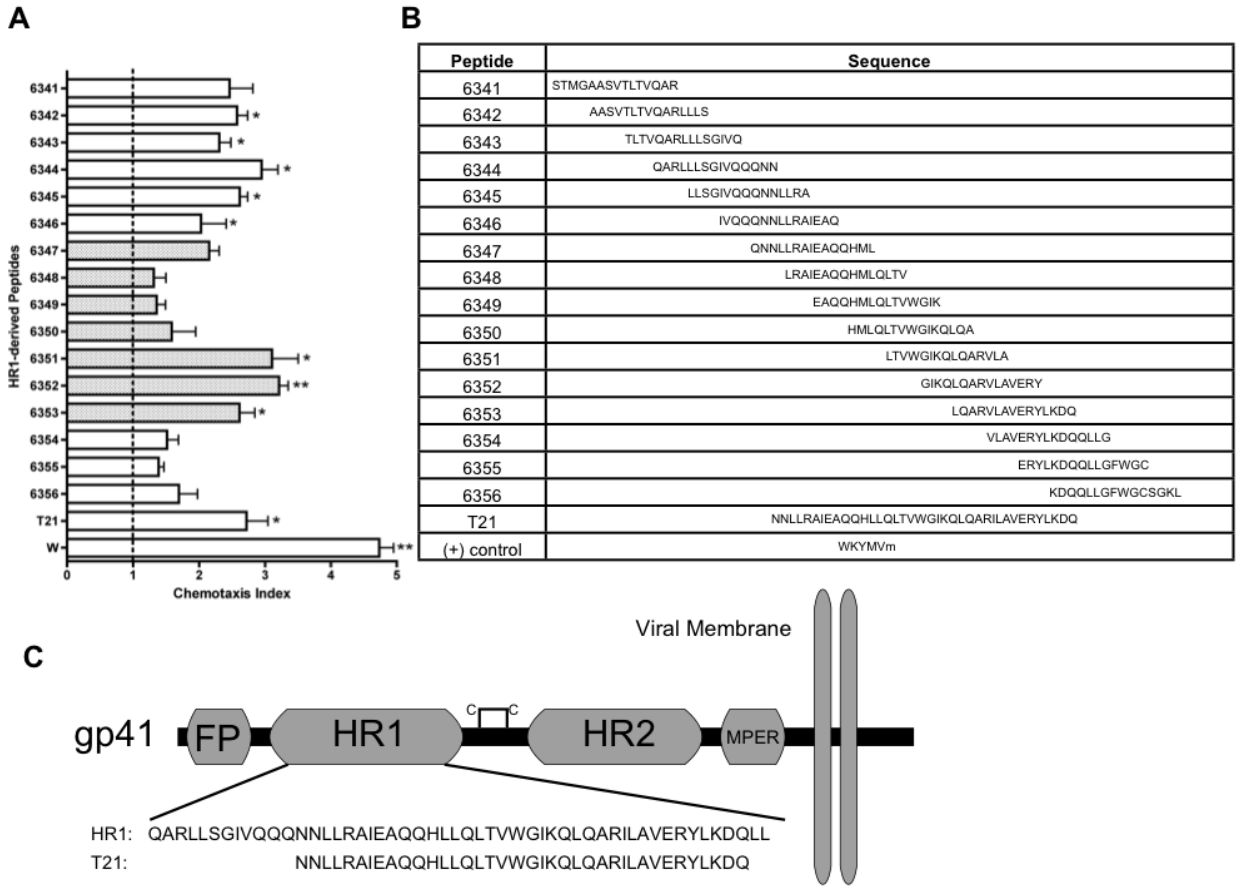

Figure 11: Chemotactic Activity of gp41 is localized in two distinct regions.

(**A**) Chemotactic activity of gp41-derived peptides was quantified to determine chemotactic regions of the gp41 HR1 helix. HL-60 neutrophil migration was assessed in response to 15 overlapping 15-mer peptides, T21, and the positive control WKYMVm. Shaded bars represent peptides that overlap with T21. Error bars represent SEM. Average cells/field from unknown and positive control conditions were compared to vehicle control to test for significant chemotaxis (N=3, * denotes $p<0.05$, ** denotes $p<0.01$). (**B**) Sequences for each peptide are listed in the table. (**C**) The regions of the gp41 ectodomain are shown with amino acid sequences of HR1 and T21 displayed beneath.

An HR1-derived peptide is specifically cleaved by matriptase to a lower molecular weight product

To determine if peptides corresponding to chemotactic regions of gp41 may be naturally produced via proteolytic processing, the HR1-derived T21 peptide was incubated with several prostate-derived proteases. Prostate specific antigen (PSA), prostasin, and matriptase were incubated with T21 and digestions were analyzed for cleavage by SDS-PAGE. We verified that our commercially-obtained PSA maintained activity by incubating it with a PSA-sensitive peptide, PAP286 20 derived from prostatic acid phosphatase (data not shown). While both PSA and prostasin failed to cleave T21, matriptase was found to effectively cleave T21 to a lower molecular weight product (**Figure 12A**). A potential matriptase cleavage product was observed at approximately 2.5 kDa. Proteolytic digestion products were then identified using MALDI-TOF mass spectrometry. Peaks corresponding to the mass of T21 remained present after treatment with PSA and prostasin (data not shown). After matriptase digestion, the T21 peak (**Figure 12B**) was completely absent and peaks corresponding to several cleavage products were present (**Figure 12C**). Sequences of cleavage products were determined based on the mass of the digested parent peptide sequence (**Figure 12D**). Based on the specificity of cleavage and peak intensity we continued to pursue the peptide with mass 2544.5 Da (MAT-1). This peptide partially overlaps with the previously characterized chemotactic sequence from our peptide library, LQARVLA, while possessing LLR/AI and QAR/IL cleavage sites at the N and C termini, respectively. The LLR and QAR residues represent the matriptase P1-P3 protease recognition sites while the hydrophobic AI and IL residues represent the P1'-P2' sites. These residues are at positions consistent with substrates commonly recognized by matriptase [82].

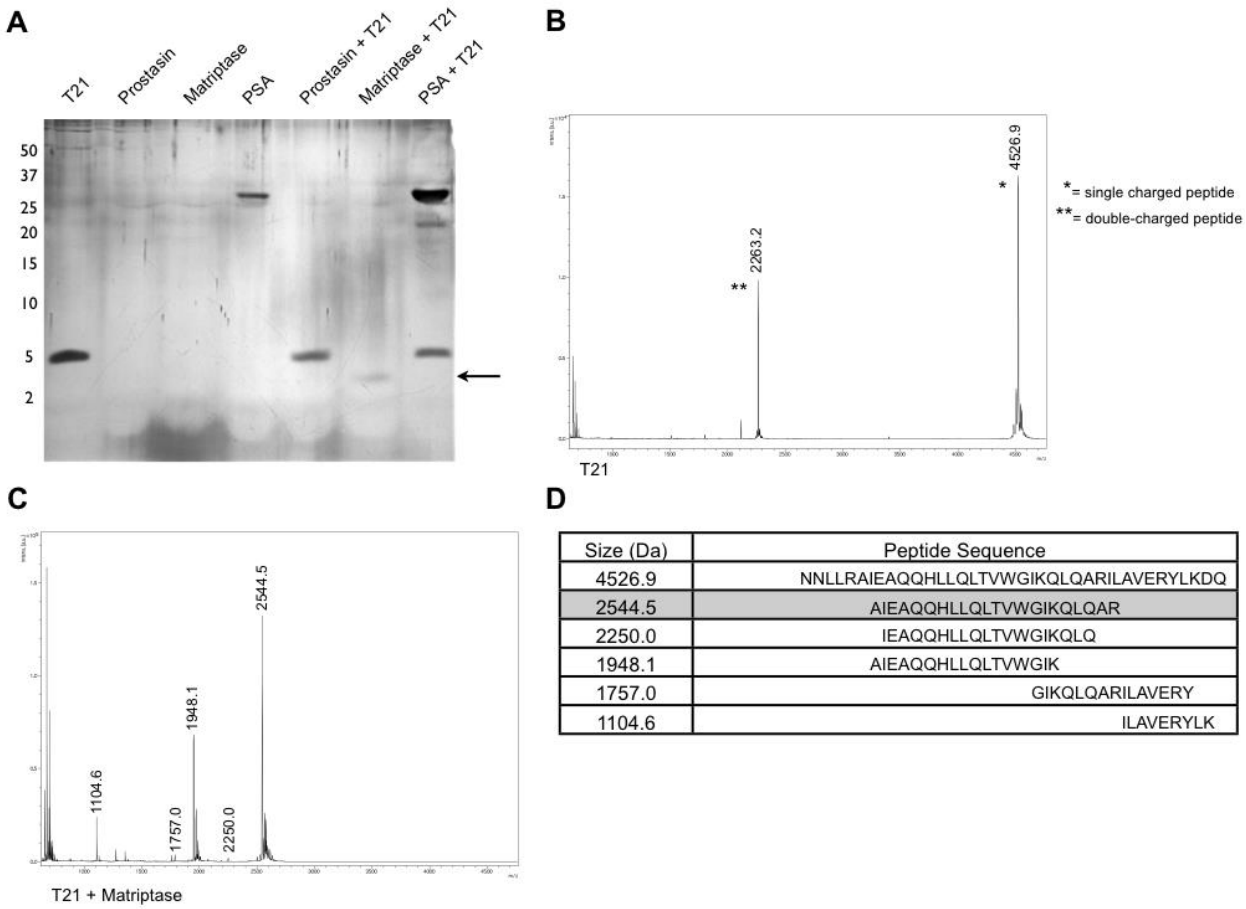

Size (Da)	Peptide Sequence
4526.9	NNLLRAIEAQQHLLQLTVWGIKQLQARILAVERYLKDQ
2544.5	AIEAQQHLLQLTVWGIKQLQAR
2250.0	IEAQQHLLQLTVWGIKQLQ
1948.1	AIEAQQHLLQLTVWGIK
1757.0	GIKQLQARILAVERY
1104.6	ILAVERYLK

Figure 12: An HR1-derived peptide is specifically cleaved by matriptase to a lower molecular weight product.

(**A**) T21 digestion reactions were resolved using SDS-PAGE and silver stained. T21 is visible as a ~5 kDa band while PSA is also visible as a ~29 kDa band. The arrow indicates the mass of the major matriptase cleavage product of T21. (**B**) Mass spectra in the peptide range (500-5000 Da) are shown for T21 alone and (**C**) matriptase + T21 conditions. Peak masses are labeled with mass [M] values reflecting the true mass of peptides. (**D**) The ExPASy FindPept tool was used to identify the sequence of peptides represented by mass peaks based on the parent T21 mass. MAT-1 is shown shaded in gray. Peaks corresponding to matriptase alone were neglected in the analysis.

Matriptase cleavage sites in gp41 are conserved across diverse HIV clades

Due to the high genetic and amino acid variation across HIV, we next assessed whether diverse HIV isolates also contained matriptase recognition sites in T21. This information would

then indicate whether matriptase cleavage is only relevant in a minority of strains, or if this is a conserved phenomenon across multiple clades of HIV. Using the most recent genetic data available from the HIV sequence compendium 28, we generated alignments of HIV-1 Group M subtype B containing 173 taxa. We then evaluated amino acid diversity across gp41 using Shannon Entropy (**Figure 13A**), which determines the variation in sequence at each amino acid position in a given alignment. This method was implemented, to measure amino acid diversity, due to overlapping coding regions within gp41 that would interfere with tests for nucleic acid diversity. Amino acids recognized by matriptase, as well as the MAT-1 peptide, were significantly conserved when compared to the entire gp41 subtype B ectodomain (**Figure 13B**).

Alignments were generated using representative DNA sequences of the gp41 ectodomain from diverse HIV clades. The phylogeny was prepared using the maximum likelihood method to show relationships between clades (**Figure 13C**). Matriptase recognition sites were found to be biochemically conserved in HIV-1 Group M, SIVcpz, and HIV-1 Group N, with a substitution of arginine 68 of gp41 with lysine in Group N. This polymorphism would be unlikely to affect the proteolytic activity of matriptase due to the preference of matriptase for both arginine and lysine residues at the P1 site 27. These findings suggest that the majority of HIV-1 strains would be susceptible to matriptase cleavage, and that our observations are not confounded by infrequent polymorphisms in the matriptase-digested peptide.

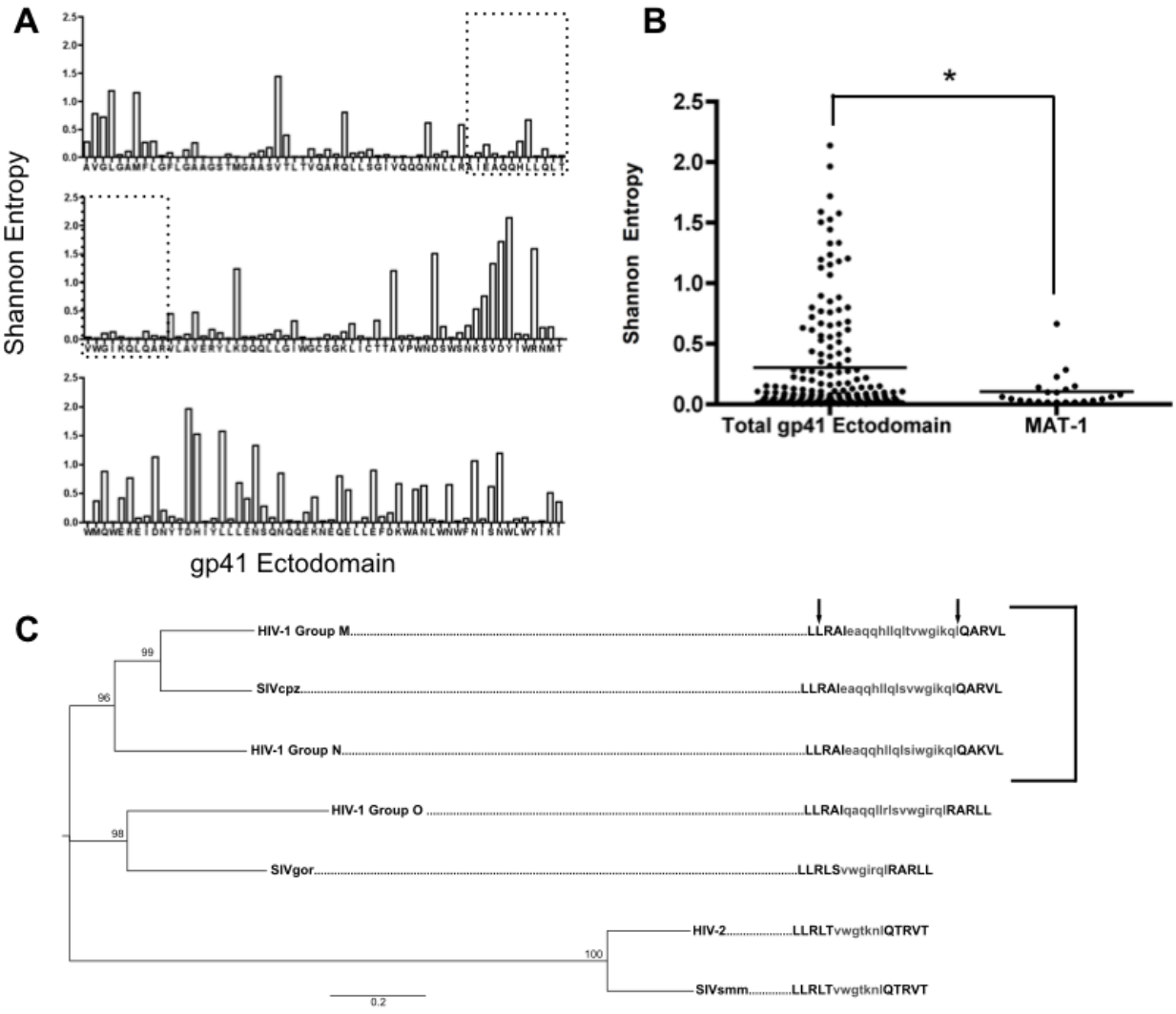

Figure 13: Matriptase cleavage sites in gp41 are conserved across diverse HIV clades.

HIV-1 Group M subtype B amino acid sequences from 173 taxa were aligned using MUSCLE. (**A**) Shannon Entropy was calculated for each amino acid spanning the gp41 ectodomain. Low values correspond to low variation and thus more conserved residues. The area enclosed in dotted boxes represents the MAT-1 peptide. (**B**) Average Entropy values for each amino acid were plotted and the median values for MAT-1 and the entire gp41 ectodomain were compared (* denotes $p<0.05$). (**C**) DNA sequences from representative strains of diverse HIV and SIV clades were aligned with ClustalW. Maximum likelihood was used to generate a phylogeny. Nodal support is represented as bootstrap values. Consensus amino acid sequences were generated for each taxa and matriptase cut sites are shown for the N and C terminals of MAT-1 as indicated by arrows. The bracketed taxa represent those containing conserved matriptase recognition sites (scale indicates 0.2 substitutions/site).

The peptide MAT-1 induces chemotaxis in primary neutrophils and monocytes and acts through FPR2

To assess the chemotactic activity of the MAT-1 cleavage product, we synthesized MAT-1 and designed experiments in primary neutrophils and monocytes using a range of peptide concentrations. The FPR2 agonist WKYMVm was used as a positive control along with a negative control peptide, RREQALLIYVA, identified by scrambling the sequence within a chemotactic region of HR1. Neutrophils were sorted from whole blood using forward and side scatter. To control for unintended stimulation, monocytes were isolated by either positive or negative selection. Positively selected monocytes were sorted from donor-derived peripheral blood mononuclear cells based on CD14 expression, while negatively sorted cells were purified by gradient centrifugation with tetrameric antibodies targeting lymphocytes. Induction of chemotaxis by MAT-1 was determined to exhibit peak activity at a concentration of 100 nM, with an average chemotaxis index of 5.4 in neutrophils (**Figure 14A**) and 2.0 and 4.4 for positively and negatively- selected monocytes, respectively (**Figure 14B and 14C**). A similar pattern of concentration-dependent activity was observed for WKYMVm. The negative peptide control exhibited no significant chemotactic activity. To assess the chemotactic activity of MAT-1 against a naturally occurring, known FPR2 agonist, equimolar concentrations cathelicidin LL-37 were compared. LL-37 has previously been shown to induce migration of several FPR2-expressing cells, including primary neutrophils and monocytes 29. At 100 nM, we observed that LL-37 and MAT-1 were equally chemotactic using primary neutrophils (**Figure 14D**).

Specificity for the receptors FPR1 and FPR2 was investigated using the peptide chemotaxis inhibitors Cyclosporin H (CSH) and WRW4, respectively (**Figure 14E**). Inhibitors were

incubated with neutrophils for 15 minutes before chemotaxis using 50 µM for WRW4 and 10 µM for CSH. MAT-1, WKYMVm, and the negative peptide control were all used at 100 nM while the FPR1-specific peptide agonist fMLP was used at 500 nM. In vehicle pretreatment conditions, chemotaxis was observed for MAT-1, WKYMVm, and fMLP. No significant chemotaxis was observed using the peptide control. After pretreatment with WRW4, chemotaxis was significantly inhibited for both MAT-1 and WKYMVm conditions. WRW4 had no significant effect on fMLP-induced neutrophil chemotaxis. Alternatively, CSH pretreatment had no significant effect on chemotaxis stimulated by MAT-1 and WKYMVm, but significantly inhibited chemotaxis in response to fMLP. Taken together, these results indicate that FPR2, but not FPR1, is necessary for the chemotactic response to MAT-1 in neutrophils.

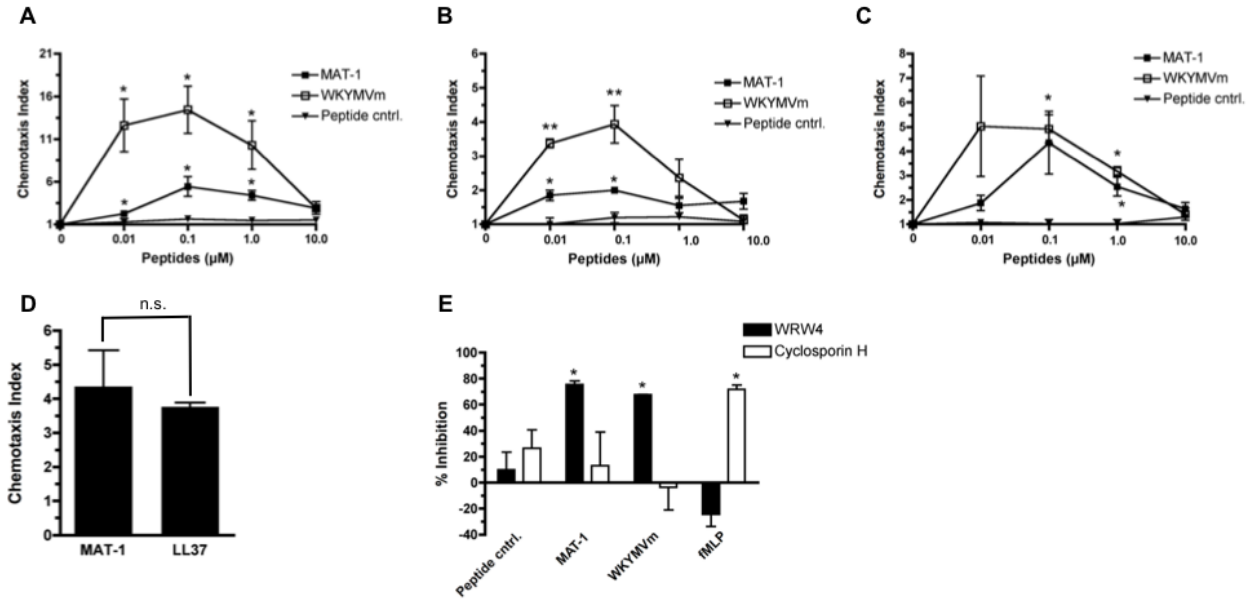

Figure 14: The peptide MAT-1 induces chemotaxis in primary neutrophils and monocytes.

Chemotaxis was assessed using increasing concentrations of peptides in primary neutrophils (**A**) and monocytes obtained by either positive selection **(B**) or negative selection (**C**). WKYMVm was used as a positive control for chemotaxis in both conditions. A negative peptide control was also used to compare to activity of MAT-1 and WKYMVm. Chemotaxis index is defined as fold change in average cells/field from media alone. Chemotaxis indexes were compared at

each concentration to a corresponding concentration of peptide control. Error bars represent SEM (N=3, * denotes p<0.05, ** denotes p<0.01). (**D**) The chemotactic activity of MAT-1 was compared to the known FPR2 agonist LL-37 using primary neutrophils. Both MAT-1 and LL-37 were used at 100 nM concentrations (n.s. denotes no significant difference). (**E**) Chemotaxis inhibitors WRW4 and Cyclosporin H were incubated for 15 minutes with neutrophils prior to determining chemotaxis in response to peptides. Chemotactic peptides were diluted to 100 nM for the control peptide, MAT-1, and WKYMVm, and 500 nM for fMLP. Percent inhibition was calculated as reduction in chemotaxis index compared to preincubation with a vehicle control. Error bars represent SEM (N=3, * denotes p<0.05).

To determine if the matriptase cleavage product MAT-1 induces chemotaxis through FPR2 alone, we generated HEK 293 cells that stably express FPR2. FPR2 expression was determined by RT-PCR (not shown), and confirmed by western analysis and flow cytometry (**Figure 15A and 15B**). While untransfected HEK 293 cells do not produce FPR2, the FPR2-transfected cells express high levels of FPR2 under the CMV promoter. Functional FPR2 activity in FPR2-HEK 293 cells was initially assessed and compared to untransfected and pcDNA3 vector control cells (**Figure 15C**). Furthermore, the MAT-1 peptide induced significant chemotaxis in FPR2-HEK 293 cells, with concentration-dependent activity (**Figure 15E**), which was absent in the scrambled peptide control. We then confirmed specificity through FPR2 by testing MAT-1 against untransfected and pcDNA-transfected cells for chemotactic activity (**Figure 15D**). These findings reveal the matriptase cleavage product MAT-1 to possess chemotactic activity directed toward FPR2 expressing cells, including primary neutrophils and monocytes.

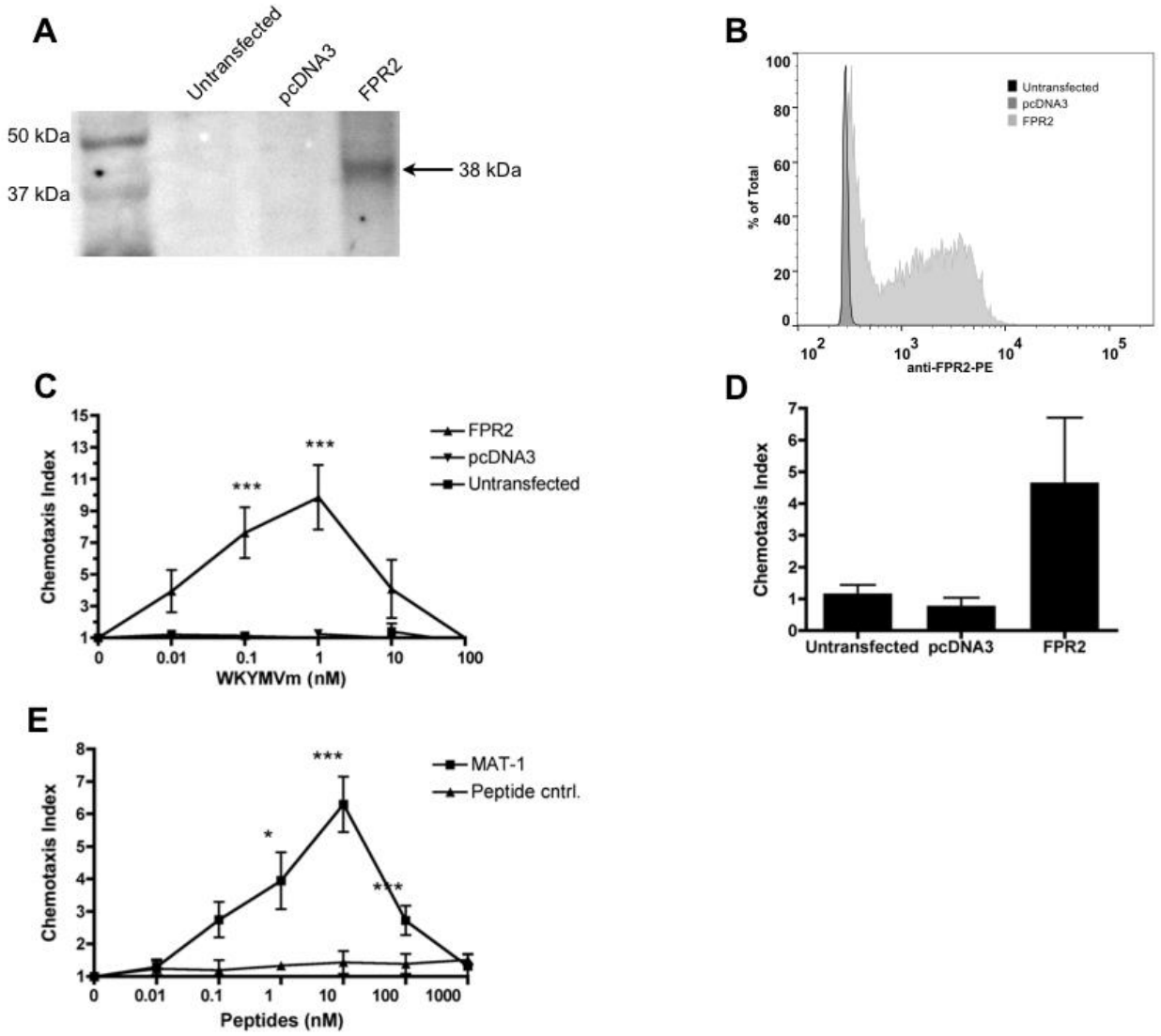

Figure 15: The peptide MAT-1 induces chemotaxis using the FPR2 receptor.

(**A**) Western blot using anti-FPR2 antibody with different HEK 293 cells shows FPR2 as a 38 kDa band. (**B**) Cytometric analysis of FPR2 expression confirms expression in FPR2-transfected cells. (**C**) Chemotaxis was assessed using increasing concentrations of WKYMVm in FPR2-transfected, pcDNA3-transfected, and untransfected HEK 293 cells. Chemotaxis indexes at each WKYMVm concentration with FPR2-expressing cells were compared to a corresponding concentration with pcDNA3 and untransfected cells. (**D**) Chemotaxis was assessed using 10 nM MAT-1 with FPR2-transfected, pcDNA3-transfected, and untransfected HEK 293 cells to confirm specificity for FPR2. (**E**) Chemotaxis assays with FPR2-transfected cells compared MAT-1 with the negative peptide control at the indicated concentrations. Error bars represent SEM (N=3, * denotes $p<0.05$, ** denotes $p<0.01$, *** denotes $p<0.001$).

Discussion

Our study presents the first evidence that chemotactic gp41 peptides are the products of proteolytic cleavage. This finding provides a physiological basis for a mechanism by which HIV can exploit the host's immunity through chemotactic regions of gp41. Monocytes and macrophages are known to express FPR2 in addition to the viral coreceptor CCR5 [83]. R5-tropic HIV, which utilizes CCR5 for entry, is predominantly responsible for infection of a new host during transmission [26]. Additionally, more recent evidence suggests that some clinical strains of R5-tropic HIV can utilize FPR2 as a coreceptor [84-86]. Thus, either by inducing migration of CCR5+ cells at the prostate epithelium or by producing chemotactic peptides that could be delivered in semen to the new host, the matriptase cleavage product identified here would be expected to promote viral transmission.

While this work demonstrates that gp41 contains conserved amino acids that are recognized as substrates by matriptase, this activity remains to be observed using intact virions. We focused our experiments on using a peptide representing the gp41 ectodomain found at the surface of the viral envelope. Therefore, the activity we observed with matriptase would be expected to be exerted upon the exposed gp41 under biological conditions. This is especially true in the case of gp120 shedding, an event that further exposes the gp41 ectodomain to the extracellular environment as "gp41 stubs" believed to function in immune evasion [87,88]. These exposed gp41 regions can act as antigens for the production of antibodies shown to enhance HIV infection [64]. Cleavage and dissemination of gp41 peptides could therefore potentially act to induce expression of these immunoevasive antibodies.

MAT-1, the most abundant matriptase cleavage product that we detected was cleaved at reported matriptase-recognition sites that we determined to be conserved across HIV-1 subtype B and represent the consensus sequence across all of HIV-1 Group M. This is significant as Group M represents >98% of all HIV-1 infections [89]. The prevalence of residues surrounding, and within, MAT-1 across diverse viral clades reflects the necessity of this region for overall viral replication. This is supported by MAT-1 being part of the leucine zipper motif of gp41, a region known to be critical for viral fusion [90]. The role of MAT-1 in transmission and infection would therefore be relevant in all but the most divergent HIV strains, accounting for <2% of infections.

This finding provides a basis for future research into how chemotactic gp41-derived peptides can affect infection while identifying matriptase as a potential target for preventing gp41-induced chemotaxis. We also have identified FPR2 as the receptor for MAT-1, which could have broad reaching effects on both pathogenesis and transmission considering the important roles of FPR2-expressing monocytes and macrophages in HIV-1 infection. Combined with previous studies with gp41-induced chemotaxis, and the evidence that FPR2 can act as a co-receptor for both lab-adapted and clinically isolated HIV-1 strains, our work supports FPR2 as a potential target for future drug development. By identifying a mechanism by which gp41 can be degraded into peptides within the host, these results promote further research into how MAT-1 and other gp41 peptide cleavage products can be produced and how they may modify host immunity.

CHAPTER 5: GENERAL DISCUSSION AND FUTURE DIRECTIONS

While increased education and access to antiretrovirals has slowed global HIV transmission, over 2 million people continue to be infected every year [1]. Microbicides offer the promise of protection in areas where there is a high rate of transmission and nonconsensual intercourse, but their success is limited by the need for affordable, mechanism-based, broad-spectrum antivirals. The challenge of microbicide development is further compounded by immense genetic diversity in HIV-1 and antiretroviral treatment leading to cross-resistance [47,53-55]. Given this information, new strategies based on a greater understanding of infection, drug susceptibility, and modulation of host immunity, will be critical for curbing the AIDS pandemic.

Here, we have provided a body of research contributing to our understanding of how HIV, and more specifically gp41, evades fusion inhibitors and modifies host immunity to promote infection. The retrocyclin RC-101 is a peptide fusion inhibitor that has been previously found to select for mutants which possess partial resistance dependent on specific mutations in gp41 [29]. How these mutations affect the activity of gp41, and how they relate to drug resistance observed in disparate fusion inhibitors is valuable to our understanding of both RC-101 and gp41. Drug resistance in transmitted HIV can potentially be countered by combining disparate antiretrovirals in a single microbicide [24]. This is demonstrated by the activity of RC-101 and CSIC against genetically diverse and drug resistance viruses. The HR1 region of gp41 has been shown to specifically induce chemotaxis in neutrophils and monocytes [61-63]. Understanding the biological importance of this finding could lead to new methods for preventing early monocyte infection and transmission at mucosal surfaces.

In Chapter 2, we observed that the same evolutionary path could achieve resistance to two distinctly different fusion inhibitors, RC-101 and ENF. Further, we described the contribution of the secondary mutation N126K, and gained a mechanistic understanding into how it could be responsible for the observed cross-resistance. These findings were then applied to demonstrate how this mutation could provide improved resistance to other unique peptide entry inhibitors. We showed for the first time that RC-101 could inhibit clinically significant ENF-resistant mutants V38A and V38+N126K. This insight provides us with direction in the continued development of fusion inhibitors and underscores the importance of compensatory HR2 mutations in drug-resistance.

One of the more interesting observations from this work was that Q66R+N126K displayed resistance to the alpha-defensin HNP-1. In addition to HNP-1, a number of other host defense peptides interfere with HIV-1 infection and replication within the host [12,91-94]. Understanding how drug resistant viruses potentially evolve cross-resistance to peptides and proteins of the innate antiviral response could help us determine the true impact of resistance to specific drugs.

The results of Chapter 3 demonstrate the potential efficacy of using RC-101 with CSIC in a microbicide to counter genetically diverse virus populations. Additionally, activity of CSIC is not compromised by mutations providing partial resistance to fusion inhibitors. The compensatory effect of combining these two mechanistically distinct drugs would overcome partial resistance afforded by the natural variation in gp41 and reverse transcriptase. In this way, developing microbicides employing RC-101 and CSIC could offer protection against a broad range of clinically occurring viruses.

While we determined that certain genetically diverse populations of HIV-1 were less susceptible to RC-101 and CSIC, demonstrated a mechanistic basis for this finding would provide useful insight into how polymorphisms frequently observed within subtypes may affect the activity of antiretroviral drugs. For example, HIV-1 subtype C has been previously shown to possess partial resistance to RC-101 [20]. These isolates contained the A67T polymorphism only identified in subtype C. Since this mutation is directly after Q66, which when mutated to R66 provides partial RC-101 resistance, it was hypothesized that A67T contributed to the reduced activity. However, the subtype C virus used in our study, 93MW960, contained the more frequently observed A67 genotype and remained less susceptible to RC-101. Additional polymorphisms in either gp41 or RT could contribute to phenotypes such as increased fusion or reduced substrate binding, respectively, which could have more broadly reaching effects on drug susceptibility. While the use of two mechanistically distinct inhibitors circumvents the problem of partial resistance to any one drug, further research is necessary to identify mutations in order to more rationally design anti-HIV compounds.

In Chapter 4, we demonstrated that the host epithelial protease, matriptase is capable of cleaving a region of gp41 to release the chemotactic MAT-1 peptide. This finding identifies matriptase as a potential target for preventing gp41-induced chemotaxis. We also have identified FPR2 as the receptor for MAT-1, which could have broad reaching effects on both pathogenesis and transmission considering the important roles of FPR2-expressing monocytes and macrophages in HIV-1 infection. Combined with previous studies with gp41-induced chemotaxis, and the evidence that FPR2 can act as a co-receptor for both lab-adapted and

clinically isolated HIV-1 strains, our work supports FPR2 as a potential target for future drug development.

Future studies involving matriptase and MAT-1 include the use of intact HIV-1 virions in enzymatic digestions. This would not only be useful in confirming that MAT-1 could indeed be produced following the interaction with matriptase and HIV-1, but these experiments, combined with comprehensive proteomics approaches utilizing mass spectrometry could help to identify additional bioactive peptides produced by gp41 digestion. Indeed, several regions of both gp120 and gp41 have been found to induce responses in leukocytes including cytokine expression and apoptosis in addition to cell migration [58-60]. Another direction for research following our findings is determining if gp41 cleavage by matriptase if sufficient to provide a direct antiviral response. Studies involving HIV-1 infection in cells expressing active matriptase on their surfaces could potentially address this hypothesis, potentially revealing matriptase to be a critical factor in mucosal anti-HIV immunity.

Together, this work advances our understanding of resistance to peptide entry inhibitors, demonstrates a potential benefit to combining specific drugs in an antiviral microbicide, and identifies a pathway by which HIV-1 may generate peptides to exploit host immunity. Our findings facilitate, not only development and application of improved anti-HIV approaches, but also provide basic mechanistic insights into HIV-1 infection. In particular, we have emphasized the importance of gp41 and its role in fusion, drug resistance, and host responses.

REFERENCES

1 Joint United Nations Programme on HIV/AIDS (UNAIDS). Global Report: UNAIDS report on the global AIDS epidemic 2013. 2013.

2 Mauck C, Ballagh S, Creinin M*, et al*. Six-day randomized safety trial of intravaginal lime juice. *J Acquir Immune Defic Syndr* 2008**; 49**:243-50.

3 Van Damme L, Ramjee G, Alary M*, et al*. Effectiveness of COL-1492, a nonoxynol-9 vaginal gel, on HIV-1 transmission in female sex workers: a randomised controlled trial. *Lancet* 2002**; 360**:971-7.

4 Lederman S, Gulick R, Chess L. Dextran sulfate and heparin interact with CD4 molecules to inhibit the binding of coat protein (gp120) of HIV. *J Immunol* 1989**; 143**:1149-54.

5 Pirrone V, Wigdahl B, Krebs F. The rise and fall of polyanionic inhibitors of the human immunodeficiency virus type 1. *Antiviral Res* 2011**; 90**:168-82.

6 McCormack S, Ramjee G, Kamali A*, et al*. PRO2000 vaginal gel for prevention of HIV-1 infection (Microbicides Development Programme 301): a phase 3, randomised, double-blind, parallel-group trial. *Lancet* 2010**; 376**:1329-37.

7 Este JA, Telenti A. HIV entry inhibitors. *Lancet* 2007**; 370**:81-88.

8 Freed EO. HIV-1 replication. *Somat Cell Mol Genet* 2001**; 26**:13-33.

9 Gallo S, Wang W, Rawat S*, et al*. Theta-defensins prevent HIV-1 Env-mediated fusion by binding gp41 and blocking 6-helix bundle formation. *J Biol Chem* 2006**; 281**:18787-92.

10 He Y, Vassell R, Zaitseva M*, et al*. Peptides trap the human immunodeficiency virus type 1 envelope glycoprotein fusion intermediate at two sites. *J Virol* 2003**; 77**:1666-1671.

11 Owen S, Rudolph D, Wang W*, et al*. RC-101, a retrocyclin-1 analogue with enhanced activity against primary HIV type 1 isolates. *AIDS Res Hum Retroviruses* 2004**; 20**:1157-65.

12 Münch J, Ständker L, Adermann K*, et al*. Discovery and optimization of a natural HIV-1 entry inhibitor targeting the gp41 fusion peptide. *Cell* 2007**; 129**:263-75.

13 D'Arrigo R, Ciccozzi M, Gori C*, et al*. gp41 sequence variability in HIV type 1 non-B subtypes infected patients undergoing enfuvirtide pressure. *AIDS Res Hum Retroviruses* 2007**; 23**:1296-1302.

14 Chinnadurai R, Munch J, Kirchhoff F. Effect of naturally-occurring gp41 HR1 variations on susceptibility of HIV-1 to fusion inhibitors. *AIDS* 2005**; 19**:1401-1405.

15 Wild CT, Shugars DC, Greenwell TK, McDanal CB, Matthews TJ. Peptides corresponding to a predictive alpha-helical domain of human immunodeficiency virus type 1 gp41 are potent inhibitors of virus infection. *Proc Natl Acad Sci U S A* 1994**; 91**:9770-9774.

16 Poveda E, Rodes B, Labernardiere JL*, et al*. Evolution of genotypic and phenotypic resistance to Enfuvirtide in HIV-infected patients experiencing prolonged virologic failure. *J Med Virol* 2004**; 74**:21-28.

17 Wei X, Decker JM, Liu H*, et al*. Emergence of resistant human immunodeficiency virus type 1 in patients receiving fusion inhibitor (T-20) monotherapy. *Antimicrob Agents Chemother* 2002**; 46**:1896-1905.

18 Cole A, Yang O, Warren A, Waring A, Lehrer R, Cole A. HIV-1 adapts to a retrocyclin with cationic amino acid substitutions that reduce fusion efficiency of gp41. *J Immunol* 2006**; 176**:6900-5.

19 Fuhrman C, Warren A, Waring A*, et al*. Retrocyclin RC-101 overcomes cationic mutations on the heptad repeat 2 region of HIV-1 gp41. *FEBS J* 2007**; 274**:6477-87.

20 Owen S, Rudolph D, Wang W*, et al*. RC-101, a retrocyclin-1 analogue with enhanced activity against primary HIV type 1 isolates. *AIDS Res Hum Retroviruses* 2004**; 20**:1157-65.

21 Cole A, Herasimtschuk A, Gupta P, Waring A, Lehrer R, Cole A. The retrocyclin analogue RC-101 prevents human immunodeficiency virus type 1 infection of a model human cervicovaginal tissue construct. *Immunology* 2007**; 121**:140-5.

22 Cole A, Patton D, Rohan L*, et al*. The formulated microbicide RC-101 was safe and antivirally active following intravaginal application in pigtailed macaques. *PLoS ONE* 2010**; 5**:e15111.

23 Cole A, Herasimtschuk A, Gupta P, Waring A, Lehrer R, Cole A. The retrocyclin analogue RC-101 prevents human immunodeficiency virus type 1 infection of a model human cervicovaginal tissue construct. *Immunology* 2007**; 121**:140-5.

24 Lederman MM, Offord RE, Hartley O. Microbicides and other topical strategies to prevent vaginal transmission of HIV. *Nat Rev Immunol* 2006**; 6**:371-382.

25 Boggiano C, Littman DR. HIV's vagina travelogue. *Immunity* 2007**; 26**:145-147.

26 Nielsen C, Pedersen C, Lundgren JD, Gerstoft J. Biological properties of HIV isolates in primary HIV infection: consequences for the subsequent course of infection. *AIDS* 1993**; 7**:1035-1040.

27 Melikyan G, Markosyan R, Hemmati H, Delmedico M, Lambert D, Cohen F. Evidence that the transition of HIV-1 gp41 into a six-helix bundle, not the bundle configuration, induces membrane fusion. *J Cell Biol* 2000**; 151**:413-23.

28 Chan D, Fass D, Berger J, Kim P. Core structure of gp41 from the HIV envelope glycoprotein. *Cell* 1997**; 89**:263-73.

29 Cole A, Yang O, Warren A, Waring A, Lehrer R, Cole A. HIV-1 adapts to a retrocyclin with cationic amino acid substitutions that reduce fusion efficiency of gp41. *J Immunol* 2006**; 176**:6900-5.

30 Owen S, Rudolph D, Wang W*, et al*. RC-101, a retrocyclin-1 analogue with enhanced activity against primary HIV type 1 isolates. *AIDS Res Hum Retroviruses* 2004**; 20**:1157-65.

31 Cole A, Patton D, Rohan L*, et al*. The formulated microbicide RC-101 was safe and antivirally active following intravaginal application in pigtailed macaques. *PLoS ONE* 2010**; 5**:e15111.

32 Cole AM, Hong T, Boo LM*, et al*. Retrocyclin: a primate peptide that protects cells from infection by T- and M-tropic strains of HIV-1. *Proc Natl Acad Sci U S A* 2002**; 99**:1813-1818.

33 Eade CR, Wood MP, Cole AM. Mechanisms and modifications of naturally occurring host defense peptides for anti-HIV microbicide development. *Curr HIV Res* 2012**; 10**:61-72.

34 Baldwin C, Sanders R, Deng Y*, et al*. Emergence of a drug-dependent human immunodeficiency virus type 1 variant during therapy with the T20 fusion inhibitor. *J Virol* 2004**; 78**:12428-37.

35 Adachi A, Gendelman HE, Koenig S*, et al*. Production of acquired immunodeficiency syndrome-associated retrovirus in human and nonhuman cells transfected with an infectious molecular clone. *J Virol* 1986**; 59**:284-291.

36 Lamers RP, Eade CR, Waring AJ, Cole AL, Cole AM. Characterization of the retrocyclin analogue RC-101 as a preventative of Staphylococcus aureus nasal colonization. *Antimicrob Agents Chemother* 2011**; 55**:5338-5346.

37 Fields GB, Noble RL. Solid phase peptide synthesis utilizing 9-fluorenylmethoxycarbonyl amino acids. *Int J Pept Protein Res* 1990**; 35**:161-214.

38 Micewicz E, Cole A, Jung C*, et al*. Grifonin-1: A Small HIV-1 Entry Inhibitor Derived from the Algal Lectin, Griffithsin. *PLoS ONE* 2010**; 5**:e14360.

39 Kimpton J, Emerman M. Detection of replication-competent and pseudotyped human immunodeficiency virus with a sensitive cell line on the basis of activation of an integrated beta-galactosidase gene. *J Virol* 1992**; 66**:2232-2239.

40 Reed, L.J., & Muench, H. A simple method for estimating fifty percent endpoints. *American Journal of Hygiene, Am J Hygiene* 1938**; 27**:493-497.

41 Miyauchi K, Kozlov MM, Melikyan GB. Early Steps of HIV-1 Fusion Define the Sensitivity to Inhibitory Peptides That Block 6-Helix Bundle Formation. *PLoS Pathog* 2009**; 5**:e1000585.

42 Baldwin C, Berkhout B. Mechanistic studies of a T20-dependent human immunodeficiency virus type 1 variant. *J Virol* 2008**; 82**:7735-40.

43 Caffrey M. Model for the structure of the HIV gp41 ectodomain: insight into the intermolecular interactions of the gp41 loop. *Biochim Biophys Acta* 2001**; 1536**:116-122.

44 Chang T, Vargas J, DelPortillo A, Klotman M. Dual role of alpha-defensin-1 in anti-HIV-1 innate immunity. *J Clin Invest* 2005**; 115**:765-73.

45 Furci L, Sironi F, Tolazzi M, Vassena L, Lusso P. Alpha-defensins block the early steps of HIV-1 infection: interference with the binding of gp120 to CD4. *Blood* 2007**; 109**:2928-35.

46 Trivedi VD, Cheng SF, Wu CW, Karthikeyan R, Chen CJ, Chang DK. The LLSGIV stretch of the N-terminal region of HIV-1 gp41 is critical for binding to a model peptide, T20. *Protein Eng* 2003**; 16**:311-317.

47 Eggink D, Baldwin CE, Deng Y*, et al*. Selection of T1249-resistant human immunodeficiency virus type 1 variants. *J Virol* 2008**; 82**:6678-6688.

48 Liu Z, Shan M, Li L*, et al*. In vitro selection and characterization of HIV-1 variants with increased resistance to sifuvirtide, a novel HIV-1 fusion inhibitor. *J Biol Chem* 2011**; 286**:3277-3287.

49 Ray N, Blackburn L, Doms R. HR-2 Mutations in Human Immunodeficiency Virus Type 1 gp41 Restore Fusion Kinetics Delayed by HR-1 Mutations That Cause Clinical Resistance to Enfuvirtide. *J Virol* 2009**; 83**:2989-2995.

50 Reeves J, Gallo S, Ahmad N*, et al*. Sensitivity of HIV-1 to entry inhibitors correlates with envelope/coreceptor affinity, receptor density, and fusion kinetics. *Proc Natl Acad Sci USA* 2002**; 99**:16249-54.

51 Reis MN, de Alcantara KC, Cardoso LP, Stefani MM. Polymorphisms in the HIV-1 gp41 env gene, natural resistance to enfuvirtide (T-20) and pol resistance among pregnant Brazilian women. *J Med Virol* 2014**; 86**:8-17.

52 Leung PH, Chen JH, Wong KH*, et al*. High prevalence of primary Enfuvirtide (ENF) resistance-associated mutations in HIV-1-infected patients in Hong Kong. *J Clin Virol* 2010**; 47**:273-275.

53 Das K, Arnold E. HIV-1 reverse transcriptase and antiviral drug resistance. Part 1. *Curr Opin Virol* 2013**; 3**:111-118.

54 Taylor BS, Sobieszczyk ME, McCutchan FE, Hammer SM. The challenge of HIV-1 subtype diversity. *N Engl J Med* 2008**; 358**:1590-1602.

55 Eggink D, Bontjer I, Langedijk JP, Berkhout B, Sanders RW. Resistance of human immunodeficiency virus type 1 to a third-generation fusion inhibitor requires multiple

mutations in gp41 and is accompanied by a dramatic loss of gp41 function. *J Virol* 2011**;** **85**:10785-10797.

56 Wood MP, Cole AL, Ruchala P*, et al*. A compensatory mutation provides resistance to disparate HIV fusion inhibitor peptides and enhances membrane fusion. *PLoS One* 2013**;** **8**:e55478.

57 Motakis D, Parniak MA. A tight-binding mode of inhibition is essential for anti-human immunodeficiency virus type 1 virucidal activity of nonnucleoside reverse transcriptase inhibitors. *Antimicrob Agents Chemother* 2002**; 46**:1851-1856.

58 Bloch I, Quintana F, Gerber D, Cohen T, Cohen I, Shai Y. T-cell inactivation and immunosuppressive activity induced by HIV gp41 via novel interacting motif. *FASEB J* 2007**;** **21**:393-401.

59 Garg H, Blumenthal R. Role of HIV Gp41 mediated fusion/hemifusion in bystander apoptosis. *Cell Mol Life Sci* 2008**; 65**:3134-44.

60 Morozov V, Morozov A, Semaan M, Denner J. Single mutations in the transmembrane envelope protein abrogate the immunosuppressive property of HIV-1. *Retrovirology* 2012**; 9**:67.

61 Le Y, Jiang S, Hu J*, et al*. N36, a synthetic N-terminal heptad repeat domain of the HIV-1 envelope protein gp41, is an activator of human phagocytes. *Clin Immunol* 2000**; 96**:236-42.

62 de Paulis A, Florio G, Prevete N*, et al*. HIV-1 envelope gp41 peptides promote migration of human Fc epsilon RI+ cells and inhibit IL-13 synthesis through interaction with formyl peptide receptors. *J Immunol* 2002**; 169**:4559-67.

63 Su S, Gao J, Gong W*, et al*. T21/DP107, A synthetic leucine zipper-like domain of the HIV-1 envelope gp41, attracts and activates human phagocytes by using G-protein-coupled formyl peptide receptors. *J Immunol* 1999**; 162**:5924-30.

64 Robinson W, Gorny M, Xu J, Mitchell W, Zolla-Pazner S. Two immunodominant domains of gp41 bind antibodies which enhance human immunodeficiency virus type 1 infection in vitro. *J Virol* 1991**; 65**:4169-76.

65 Burrer R, Haessig-Einius S, Aubertin A, Moog C. Neutralizing as well as non-neutralizing polyclonal immunoglobulin (Ig)G from infected patients capture HIV-1 via antibodies directed against the principal immunodominant domain of gp41. *Virology* 2005**; 333**:102-13.

66 Le Tortorec A, Satie A, Denis H*, et al*. Human prostate supports more efficient replication of HIV-1 R5 than X4 strains ex vivo. *Retrovirology* 2008**; 5**:119.

67 Smith D, Kingery J, Wong J, Ignacio C, Richman D, Little S. The prostate as a reservoir for HIV-1. *AIDS* 2004**; 18**:1600-2.

68 Eisele E, Siliciano R. Redefining the viral reservoirs that prevent HIV-1 eradication. *Immunity* 2012**; 37**:377-88.

69 Chun T, Fauci A. HIV reservoirs: pathogenesis and obstacles to viral eradication and cure. *AIDS* 2012**; 26**:1261-8.

70 Lawless MK, Barney S, Guthrie KI, Bucy TB, Petteway SR,Jr, Merutka G. HIV-1 membrane fusion mechanism: structural studies of the interactions between biologically-active peptides from gp41. *Biochemistry* 1996**; 35**:13697-13708.

71 Millius A, Weiner O. Chemotaxis in neutrophil-like HL-60 cells. *Methods Mol Biol* 2009**; 571**:167-77.

72 Collins SJ, Ruscetti FW, Gallagher RE, Gallo RC. Normal functional characteristics of cultured human promyelocytic leukemia cells (HL-60) after induction of differentiation by dimethylsulfoxide. *J Exp Med* 1979**; 149**:969-974.

73 Livak KJ, Schmittgen TD. Analysis of relative gene expression data using real-time quantitative PCR and the 2(-Delta Delta C(T)) Method. *Methods* 2001**; 25**:402-408.

74 Pryde J. Partitioning of proteins in Triton X-114. *Methods Mol Biol* 1998**; 88**:23-33.

75 Martellini JA, Cole AL, Venkataraman N*, et al*. Cationic polypeptides contribute to the anti-HIV-1 activity of human seminal plasma. *FASEB J* 2009**; 23**:3609-3618.

76 Chen LM, Skinner ML, Kauffman SW*, et al*. Prostasin is a glycosylphosphatidylinositol-anchored active serine protease. *J Biol Chem* 2001**; 276**:21434-21442.

77 Martellini J, Cole A, Svoboda P*, et al*. HIV-1 enhancing effect of prostatic acid phosphatase peptides is reduced in human seminal plasma. *PLoS ONE* 2011**; 6**:e16285.

78 Tamura K, Peterson D, Peterson N, Stecher G, Nei M, Kumar S. MEGA5: molecular evolutionary genetics analysis using maximum likelihood, evolutionary distance, and maximum parsimony methods. *Mol Biol Evol* 2011**; 28**:2731-2739.

79 Boulay F, Tardif M, Brouchon L, Vignais P. The human N-formylpeptide receptor. Characterization of two cDNA isolates and evidence for a new subfamily of G-protein-coupled receptors. *Biochemistry* 1990**; 29**:11123-33.

80 Murphy P, Ozçelik T, Kenney R, Tiffany H, McDermott D, Francke U. A structural homologue of the N-formyl peptide receptor. Characterization and chromosome mapping of a peptide chemoattractant receptor family. *J Biol Chem* 1992**; 267**:7637-43.

81 Le Y, Gong W, Li B*, et al*. Utilization of two seven-transmembrane, G protein-coupled receptors, formyl peptide receptor-like 1 and formyl peptide receptor, by the synthetic hexapeptide WKYMVm for human phagocyte activation. *J Immunol* 1999**; 163**:6777-6784.

82 Beliveau F, Desilets A, Leduc R. Probing the substrate specificities of matriptase, matriptase-2, hepsin and DESC1 with internally quenched fluorescent peptides. *FEBS J* 2009**; 276**:2213-2226.

83 Le Y, Yang Y, Cui Y*, et al*. Receptors for chemotactic formyl peptides as pharmacological targets. *Int Immunopharmacol* 2002**; 2**:1-13.

84 Nedellec R, Coetzer M, Shimizu N*, et al*. Virus entry via the alternative coreceptors CCR3 and FPRL1 differs by human immunodeficiency virus type 1 subtype. *J Virol* 2009**; 83**:8353-63.

85 Shimizu N, Tanaka A, Mori T*, et al*. A formylpeptide receptor, FPRL1, acts as an efficient coreceptor for primary isolates of human immunodeficiency virus. *Retrovirology* 2008**; 5**:52.

86 Shimizu N, Tanaka A, Oue A*, et al*. Broad usage spectrum of G protein-coupled receptors as coreceptors by primary isolates of HIV. *AIDS* 2009**; 27**:761-9.

87 Moore JP, McKeating JA, Weiss RA, Sattentau QJ. Dissociation of gp120 from HIV-1 virions induced by soluble CD4. *Science* 1990**; 250**:1139-1142.

88 Crooks ET, Tong T, Osawa K, Binley JM. Enzyme digests eliminate nonfunctional Env from HIV-1 particle surfaces, leaving native Env trimers intact and viral infectivity unaffected. *J Virol* 2011**; 85**:5825-5839.

89 Sharp PM, Hahn BH. Origins of HIV and the AIDS pandemic. *Cold Spring Harb Perspect Med* 2011**; 1**:a006841.

90 Chan D, Fass D, Berger J, Kim P. Core structure of gp41 from the HIV envelope glycoprotein. *Cell* 1997**; 89**:263-73.

91 Quiñones-Mateu M, Lederman M, Feng Z*, et al*. Human epithelial beta-defensins 2 and 3 inhibit HIV-1 replication. *AIDS* 2003**; 17**:F39-48.

92 Dürr U, Sudheendra U, Ramamoorthy A. LL-37, the only human member of the cathelicidin family of antimicrobial peptides. *Biochimica et Biophysica Acta (BBA) - Biomembranes* 2006**; 1758**:1408-1425.

93 Johansson J, Gudmundsson G, Rottenberg M, Berndt K, Agerberth B. Conformation-dependent antibacterial activity of the naturally occurring human peptide LL-37. *J Biol Chem* 1998**; 273**:3718-24.

94 Wu Z, Cocchi F, Gentles D*, et al*. Human neutrophil alpha-defensin 4 inhibits HIV-1 infection in vitro. *FEBS Letters* 2005**; 579**:162-6.